

# Nonequilibrium thermodynamics of the asymmetric Sherrington-Kirkpatrick model

Miguel Aguilera\*

*School of Engineering and Informatics  
University of Sussex  
Falmer, Brighton. United Kingdom*

Masanao Igarashi†

*Department of Applied Physics,  
Graduate School of Engineering, Hokkaido University  
Sapporo, Japan*

Hideaki Shimazaki‡

*Center for Human Nature, Artificial Intelligence,  
and Neuroscience (CHAIN), Hokkaido University  
Sapporo, Japan*

(Dated: May 23, 2022)

Most systems in nature operate far from equilibrium, displaying time-asymmetric, irreversible dynamics. When a system's elements are numerous, characterizing its nonequilibrium states is challenging due to the expansion of its state space. Inspired by the success of the equilibrium Ising model in investigating disordered systems in the thermodynamic limit, we study the nonequilibrium thermodynamics of the asymmetric Sherrington-Kirkpatrick system as a prototypical model of large-scale nonequilibrium processes. We employ a path integral method to calculate a generating functional over the trajectories to derive exact solutions of the order parameters, conditional entropy of trajectories, and steady-state entropy production of infinitely large networks. The order parameters reveal order-disorder nonequilibrium phase transitions as found in equilibrium systems but no dynamics akin to the spin-glass phase. We find that the entropy production peaks at the phase transition, but it is more prominent outside the critical regime, especially for disordered phases with low entropy rates. While entropy production is becoming popular to characterize various complex systems, our results reveal that increased entropy production is linked with radically different scenarios, and combining multiple thermodynamic quantities yields a more precise picture of a system. These results contribute to an exact analytical theory for studying the thermodynamic properties of large-scale nonequilibrium systems and their phase transitions.

## I. INTRODUCTION

While isolated systems tend toward thermodynamic equilibrium, many physical, chemical, and biological processes operate far from equilibrium. Such nonequilibrium systems persist by exchanging matter and energy with their surroundings while the systems are driven by time-varying external stimuli or causally by their past states. In consequence, interaction of systems with their environment (from molecules to organisms and machines) are inherently nonequilibrium processes, where e.g., adaptive action of sensor and effector interfaces break time reversal symmetry [1]. Nonequilibrium interactions result in temporally irreversible patterns strikingly different from the reversible dynamics found at thermodynamic equilibrium. Understanding these dissipative processes—describing spatial and temporal patterns with a definite past-future order, e.g., chemical reactions, neural dynamics, or flocks of birds—brings critical insights into how open systems self-organize [2]. Although these

ideas have attracted the interest of disparate fields from evolutionary dynamics [3] to neuroscience [4–7], little is known about the thermodynamic description of nonequilibrium systems comprising many interacting particles. While stochastic thermodynamics has been greatly influential for the study of small systems interacting with their surroundings [8], the thermodynamics of large-scale nonequilibrium systems and their phase transitions have attracted attention only very recently [9–11].

In this paper, we study the nonequilibrium thermodynamics of a stochastic, kinetic Ising model. The Ising model is a cornerstone of statistical mechanics, originally conceived as a model describing phase transitions in magnetic materials [12]. A natural extension of the model introducing Markovian dynamics is the kinetic Ising model, a prototypical model of both equilibrium and nonequilibrium systems, such as recurrent neural networks [13] or genetic regulatory networks [14]. With symmetric couplings and time-independent external fields, the kinetic Ising model results in an equilibrium process exhibiting a variety of complex phenomena, including ordered (ferromagnetic), disordered (paramagnetic), and quenched disordered states (known as spin glasses). The celebrated Sherrington-Kirkpatrick (SK) model, characterized by quenched random couplings, is a solvable model includ-

\* sci@maguilera.net

† igarashim@eng.hokudai.ac.jp

‡ shimazaki@chain.hokudai.ac.jp

ing a spin-glass phase [15]. The equilibrium solution of the SK model can be derived using the replica mean-field method [12, 16]. A kinetic version of this symmetric-coupling model has been represented as a bipartite network, also solved using the replica trick [17].

In symmetrically coupled networks without varying fields, the kinetics of the Ising systems seen forward or backward (known as reversing the arrow of time) are indistinguishable. This time-symmetry breaks down under time-varying external fields or asymmetric couplings comprising history-dependent, non-conservative forces, resulting in nonequilibrium processes where the detailed balance is violated. In the latter case, the system may relax towards a steady-state known as the nonequilibrium steady state after some time. While a nonequilibrium system will have a non-negative entropy production [8, 18–20], the system may maintain structured states by dissipating the heat to the reservoirs [2]. Under ‘local detailed balance’, a system coupled to equilibrium reservoirs or *heat baths* [21, 22], these time-asymmetric trajectories are linked with the heat transferred to the reservoirs or entropy change of the heat baths. In particular, under the steady-state conditions, the entropy production is identical to this entropy change of the heat bath (dissipated entropy to the reservoir), and the *house-keeping* entropy production [23, 24] that quantifies violation of the detailed balance caused by the non-conservative forces. The steady-state entropy production is thus critical to unveiling the interaction of out-of-equilibrium systems with their environments. Yet, unlike its equilibrium counterpart, the properties of the irreversible Ising dynamics remain unclear as its entropy production has not been underpinned theoretically [25, 26].

Here, we study the kinetics of the SK model with asymmetric connections as a prototypical model of nonlinear and nonequilibrium processes. As the model does not have an equilibrium distribution or a free energy defined in classical terms as the equilibrium SK model, we recur to a dynamical equivalent in the form of a generating functional. We apply a path integral approach to exactly calculate a generating functional over the system’s trajectories, capturing its sufficient statistics and nonequilibrium thermodynamic descriptions. Unlike the replica method, the generating functional for fully asymmetric couplings has exact solutions in the thermodynamic limit without additional assumptions like analytic continuation and replica symmetry breaking [27].

One of the open questions in empirical studies is whether nonequilibrium dynamics and its large entropy production are linked with the critical properties of systems operating near continuous phase transitions [5, 6]. Naive mean-field approximations of simple nonequilibrium systems support this assumption. For example, the entropy production of an Ising model with an oscillatory field or a mean-field majority vote model peaks around a critical point [28–30]. In the stationary kinetic Ising model, by applying mean-field approximations preserving fluctuations in the system, we also showed that

the entropy production takes a maximum around a critical point [31]. All these results rely on approximations; therefore the assumption that entropy production is maximized near the continuous phase transitions has not yet been ratified by exact solutions of spin models in the thermodynamic limit. In this study, we find that the entropy production is locally maximized at critical phase transition points. This result supports the use of entropy production to investigate the criticality of systems, where the free energy or heat capacity is not defined globally. Nevertheless, we also show that entropy production can take larger values for considerably heterogeneous couplings under low-temperature regimes, where the system shows disordered but highly deterministic dynamics. Thus, one must examine the entropy production carefully, as its large magnitude does not necessarily mean that the system is in a critical state. Instead, we propose that combining the entropy rate and entropy production yields a more precise picture of order-disorder continuous phase transitions.

The paper organizes as follows. In Section II, we present a general introduction of the maximum entropy discrete Markov processes to which the kinetic Ising model belongs and discuss its entropy production. We then introduce a generating functional of the process to compute the entropy production and the statistical moments of the system. A path integral method calculating the configurational average of the generating functional is given in Section IV, where we derive an exact mean-field solution of the entropy production, magnetization, and correlations in an infinite system. In Section V, we compute phase maps of the order parameters and entropy production using these theoretical results with and without randomly sampled external fields. We investigate the critical line for the nonequilibrium phase transitions and its relation to the entropy production. In Section VI, we close the paper with implications of our results for the analyses of biological systems.

## II. MAXIMUM ENTROPY MARKOV CHAINS, ENTROPY PRODUCTION, AND GENERATING FUNCTIONAL

### A. Maximum entropy Markov chains

The principle of maximum entropy is a foundation of equilibrium statistical mechanics [32]. The principle has been later generalized for treating time-dependent phenomena, sometimes referred to as the principle of maximum caliber or maximum path entropy [33, 34]. Under consistency requirements preserving causal interactions, the application of the maximum caliber principle yields a Markov process, defining transition probabilities related to Lagrange multipliers under maximum path entropy [35], also coinciding with the method of maximum likelihood estimation. To see this, let us start with a discrete-time stochastic process whose discrete state space of  $N$

elements at time  $u$  is given by  $\mathbf{s}_u = \{s_{1,u}, \dots, s_{N,u}\}$ . Consider its trajectories of length  $t+1$ , and denote the probability for the trajectory by  $p(\mathbf{s}_{0:t})$ . The path entropy is defined as

$$S_{0:t} = - \sum_{\mathbf{s}_{0:t}} p(\mathbf{s}_{0:t}) \log p(\mathbf{s}_{0:t}). \quad (1)$$

Maximizing the equation above, subject to constraints, gives the least structured distribution  $p(\mathbf{s}_{0:t})$  consistent with observations [36]. Nevertheless, given a set of constraints, the maximum entropy distributions for overlapping paths can result in different functions when marginalized to the same section of the path. Thus, in order to model causal networks, entropy maximization has to be constrained with a set of temporal consistency requirements [35], as was first established by [37]. Specifically, for any positive integer  $u (\leq t)$ , we impose

$$\sum_{\mathbf{s}_{u+1}} p^{(u+1)}(\mathbf{s}_{0:u+1}) = p^{(u)}(\mathbf{s}_{0:u}), \quad (2)$$

where  $p^{(u)}(\mathbf{s}_{0:u})$  is given by

$$p^{(u)}(\mathbf{s}_{0:u}) = \arg \max_{p(\mathbf{s}_{0:u})} S_{0:u}. \quad (3)$$

Namely, the marginal probability distribution for the maximum entropy path  $\mathbf{s}_{0:u}$  in  $p(\mathbf{s}_{0:u+1})$  is consistent with the probability distribution for the maximum entropy path  $\mathbf{s}_{0:u}$  of  $p(\mathbf{s}_{0:u})$ . Constraining path distributions with dependencies only between consecutive states (i.e., transition probabilities only depend on the present state), maximization of Eq. 1 with a set of constraints  $f_n(\mathbf{s}_u, \mathbf{s}_{u-1}) = C_u^n$  under an initial distribution  $p(\mathbf{s}_0)$  and the consistency condition in Eq. 2 results in (cf. [35])

$$\begin{aligned} p(\mathbf{s}_{0:t}) &= p(\mathbf{s}_0) \prod_{u=1}^t p(\mathbf{s}_u | \mathbf{s}_{u-1}) \\ &\propto p(\mathbf{s}_0) \prod_{u=1}^t \exp \left[ \sum_n \lambda_n f_n(\mathbf{s}_u, \mathbf{s}_{u-1}) \right]. \end{aligned} \quad (4)$$

That is, a stochastic process consistent with the maximum caliber is a Markovian process.

The path entropy can be then decomposed into

$$\begin{aligned} S_{0:t} &= \sum_{\mathbf{s}_{0:t}} p(\mathbf{s}_{0:t}) \left( \sum_u -\log p(\mathbf{s}_u | \mathbf{s}_{u-1}) - \log p(\mathbf{s}_0) \right) \\ &= \sum_u S_{u|u-1} + S_0, \end{aligned} \quad (5)$$

where  $S_0$  is the entropy of the initial distribution and  $S_{u|u-1}$  is a conditional entropy, defined as

$$S_{u|u-1} = - \sum_{\mathbf{s}_u, \mathbf{s}_{u-1}} p(\mathbf{s}_u, \mathbf{s}_{u-1}) \log p(\mathbf{s}_u | \mathbf{s}_{u-1}), \quad (6)$$

which at the steady state corresponds to the Kolmogorov–Sinai entropy or entropy rate,  $\lim_{t \rightarrow \infty} \frac{1}{t} S_{0:t}$ .

## B. Steady-state entropy production

In stochastic processes in thermodynamic equilibrium, forward and time-reversed trajectories are indistinguishable. Markov processes can break this time-reversal symmetry, capturing the irreversible characteristics of physical and biological processes [38]. Stochastic thermodynamics proposes a link between the time-irreversible stochastic trajectories with surroundings in the form of heat (entropy) dissipation. To see this, we dissect the system's entropy as follows.

As the system evolves, it experiences an entropy change  $\sigma_u^{\text{sys}}$ :

$$\sigma_u^{\text{sys}} = S_u - S_{u-1} = \sum_{\mathbf{s}_u, \mathbf{s}_{u-1}} p(\mathbf{s}_u, \mathbf{s}_{u-1}) \log \frac{p(\mathbf{s}_{u-1})}{p(\mathbf{s}_u)}. \quad (7)$$

Here  $p(\mathbf{s}_u)$  is a marginal probability distribution of elements at time  $u$ . Nonequilibrium systems may maintain irreversible dynamics by continuously dissipating heat (entropy) to their environments. Under the local detailed balance [21, 22, 39] for a system coupled to a heat bath, the entropy change results from subtraction of the entropy dissipated to the heat bath,  $\sigma_u^{\text{bath}}$ , from the (total) entropy production,  $\sigma_u$ :

$$\sigma_u^{\text{sys}} = \sigma_u - \sigma_u^{\text{bath}}, \quad (8)$$

where the entropy change of the heat bath is given as

$$\sigma_u^{\text{bath}} = \sum_{\mathbf{s}_u, \mathbf{s}_{u-1}} p(\mathbf{s}_u, \mathbf{s}_{u-1}) \log \frac{p(\mathbf{s}_u | \mathbf{s}_{u-1})}{p(\mathbf{s}_{u-1} | \mathbf{s}_u)}, \quad (9)$$

where  $p(\mathbf{s}_{u-1} | \mathbf{s}_u)$  is a transition probability (from Eq. 4) but evaluated by the reverse trajectory [21, 40], that is, we define it using the transition function at time  $u$ , but switching  $\mathbf{s}_u$  and  $\mathbf{s}_{u-1}$ . This equation relates the system's time asymmetry with the entropy change of the reservoir.

The entropy production  $\sigma_u$  at time  $u$  is then given as

$$\sigma_u = \sum_{\mathbf{s}_u, \mathbf{s}_{u-1}} p(\mathbf{s}_u, \mathbf{s}_{u-1}) \log \frac{p(\mathbf{s}_u | \mathbf{s}_{u-1}) p(\mathbf{s}_{u-1})}{p(\mathbf{s}_{u-1} | \mathbf{s}_u) p(\mathbf{s}_u)}, \quad (10)$$

which is the Kullback-Leibler divergence between the forward and backward trajectories [8, 18, 20, 41]. Due to the non-negativity of the divergence, the entropy production is non-negative,  $\sigma_u \geq 0$ . This entropy production vanishes if the probability of forward trajectories from the future states is identical to a posterior of the past state given the future state [20], i.e., when the process loses time-asymmetry in prediction and postdiction [42].

In a steady state, where  $\sigma_u^{\text{sys}} = 0$ , the entropy production is caused by the dissipation only, and becomes equivalent to the entropy change of the heat bath, which can be represented as

$$\sigma_u = \sigma_u^{\text{bath}} = -S_{u|u-1} + S_{u|u-1}^r. \quad (11)$$

Here  $S_{u|u-1}^r$  is the entropy of the time-reversed conditional distribution:

$$S_{u|u-1}^r \equiv - \sum_{\mathbf{s}_u, \mathbf{s}_{u-1}} p(\mathbf{s}_u, \mathbf{s}_{u-1}) \log p(\mathbf{s}_{u-1} | \mathbf{s}_u). \quad (12)$$

The steady-state entropy production in this form is also equivalent to the *house-keeping* entropy production caused by the non-conservative forces under a steady state [23, 24]. In general, the non-zero house-keeping entropy production results in the violation of the detailed balance  $p(\mathbf{s}_u | \mathbf{s}_{u-1}) p^{\text{ss}}(\mathbf{s}_{u-1}) = p(\mathbf{s}_{u-1} | \mathbf{s}_u) p^{\text{ss}}(\mathbf{s}_u)$ , where  $p^{\text{ss}}(\mathbf{s}_u)$  is the steady-state distribution [43], making the process out-of-equilibrium. Thus, in the steady state, non-zero entropy production is a hallmark of a nonequilibrium process that is interacting with the environment. In this study, we examine this steady-state entropy production (Eq. 11).

### C. Generating functional and nonequilibrium statistics

Consider the maximum caliber distribution (Eq. 4) of  $N$  interacting elements  $\mathbf{s}_u = \{s_{1,u}, \dots, s_{N,u}\}$ , we investigate statistical properties of the system at each time step expected from the ensemble of the history-dependent trajectories given by the path distribution

$$\begin{aligned} p(\mathbf{s}_{0:t}) &= \prod_{u=1}^t p(\mathbf{s}_u | \mathbf{s}_{u-1}) p(\mathbf{s}_0) \\ &= \sum_{\mathbf{s}_{0:t}} \exp \left[ - \sum_u \epsilon(\mathbf{s}_u | \mathbf{s}_{u-1}) \right] p(\mathbf{s}_0), \end{aligned} \quad (13)$$

where  $\epsilon(\mathbf{s}_u | \mathbf{s}_{u-1}) \equiv -\log p(\mathbf{s}_u | \mathbf{s}_{u-1})$ . Using the above equation, we define means and (equal-time and delayed) correlations of the states as:

$$m_{i,u} = \sum_{\mathbf{s}_{0:t}} s_{i,u} p(\mathbf{s}_{0:t}) = \sum_{\mathbf{s}_u} s_{i,u} p(\mathbf{s}_u) \quad (14)$$

$$R_{ij,uv} = \sum_{\mathbf{s}_{0:t}} s_{i,u} s_{j,v} p(\mathbf{s}_{0:t}) = \sum_{\mathbf{s}_u, \mathbf{s}_v} s_{i,u} s_{j,v} p(\mathbf{s}_u, \mathbf{s}_v), \quad (15)$$

where  $p(\mathbf{s}_u), p(\mathbf{s}_u, \mathbf{s}_v)$  are the marginal densities at time  $u$  and  $v$ . As we will see, these variables underpin the order parameters of the system, consisting on means and delayed self-correlations averaged over the elements:

$$m_u = \frac{1}{N} \sum_i m_{i,u}, \quad (16)$$

$$q_{u,v} = \frac{1}{N} \sum_i R_{ii,uv}. \quad (17)$$

In addition, we wish to elucidate the entropy production under a steady state (calculated from the conditional entropy and reverse conditional entropy rates). All these quantities depend on marginal distributions, making it

difficult to calculate them as the number of possible patterns increases combinatorially with  $t$  and  $N$ .

In equilibrium systems, the partition function provides the statistical moments of the equilibrium distribution. Here, to retrieve the statistical properties of ensemble trajectories (Eqs. 14, 15, but also 6 and 12), we introduce a generating functional or dynamical partition function:

$$Z_t(\mathbf{g}) = \sum_{\mathbf{s}_{0:t}} \exp \left[ - \sum_u \epsilon(\mathbf{s}_u | \mathbf{s}_{u-1}) + \Gamma(\mathbf{g}, \mathbf{s}_{0:t}) \right] p(\mathbf{s}_0), \quad (18)$$

where

$$\begin{aligned} \Gamma(\mathbf{g}, \mathbf{s}_{0:t}) &= \sum_{i,u} g_{i,u} s_{i,u} - \sum_u g_{\sigma,u} \epsilon(\mathbf{s}_u | \mathbf{s}_{u-1}) \\ &\quad - \sum_u g_{\sigma,u}^r \epsilon(\mathbf{s}_{u-1} | \mathbf{s}_u). \end{aligned} \quad (19)$$

In the limit of  $t \rightarrow \infty$ , the logarithm of the generating functional converges to the large deviation function [44–46],

$$\lim_{t \rightarrow \infty} \frac{1}{t} \log Z_t(\mathbf{g}) = \varphi(\mathbf{g}), \quad (20)$$

which plays the role of a free-energy function for nonequilibrium trajectories [47]. The vector  $\mathbf{g}$  is composed of parameters  $g_{i,u}$ ,  $g_{\sigma,u}$ , and  $g_{\sigma,u}^r$  ( $i = 1, \dots, N$  and  $u = 1, \dots, t$ ) to retrieve different statistics of the system. The parameters  $g_{i,u}$  recover the moments of the system. We can obtain the first and second order moments (Eqs. 14 and 15) by

$$m_{i,u} = \lim_{\mathbf{g} \rightarrow \mathbf{0}} \frac{\partial Z_t(\mathbf{g})}{\partial g_{i,u}} = \lim_{\mathbf{g} \rightarrow \mathbf{0}} \langle s_{i,u} \rangle_{\mathbf{g}} = \langle s_{i,u} \rangle, \quad (21)$$

$$R_{ij,uv} = \lim_{\mathbf{g} \rightarrow \mathbf{0}} \frac{\partial^2 Z_t(\mathbf{g})}{\partial g_{i,u} \partial g_{j,v}} = \lim_{\mathbf{g} \rightarrow \mathbf{0}} \langle s_{i,u} s_{j,v} \rangle_{\mathbf{g}} = \langle s_{i,u} s_{j,v} \rangle, \quad (22)$$

where angle brackets are defined as

$$\langle f(\mathbf{s}_{0:t}) \rangle_{\mathbf{g}} = \sum_{\mathbf{s}_{0:t}} f(\mathbf{s}_{0:t}) \exp \left[ \sum_{i,u} g_{i,u} s_{i,u} \right] p(\mathbf{s}_{0:t}), \quad (23)$$

$$\langle f(\mathbf{s}_{0:t}) \rangle = \sum_{\mathbf{s}_{0:t}} f(\mathbf{s}_{0:t}) p(\mathbf{s}_{0:t}). \quad (24)$$

Moreover,  $g_{\sigma,u}$ ,  $g_{\sigma,u}^r$  retrieve the conditional and reversed conditional entropy terms  $S_{u|u-1}$ ,  $S_{u|u-1}^r$ , respectively:

$$\begin{aligned} S_{u|u-1} &= - \lim_{\mathbf{g} \rightarrow \mathbf{0}} \frac{\partial Z_t(\mathbf{g})}{\partial g_{\sigma,u}} \\ &= \lim_{\mathbf{g} \rightarrow \mathbf{0}} \langle \epsilon(\mathbf{s}_u | \mathbf{s}_{u-1}) \rangle_{\mathbf{g}} = \langle \epsilon(\mathbf{s}_u | \mathbf{s}_{u-1}) \rangle, \end{aligned} \quad (25)$$

$$\begin{aligned} S_{u|u-1}^r &= - \lim_{\mathbf{g} \rightarrow \mathbf{0}} \frac{\partial Z_t(\mathbf{g})}{\partial g_{\sigma,u}^r} \\ &= \lim_{\mathbf{g} \rightarrow \mathbf{0}} \langle \epsilon(\mathbf{s}_{u-1} | \mathbf{s}_u) \rangle = \langle \epsilon(\mathbf{s}_{u-1} | \mathbf{s}_u) \rangle. \end{aligned} \quad (26)$$

Finally, using these terms, the steady-state entropy production (Eq. 11) is given by

$$\sigma_u = \lim_{\mathbf{g} \rightarrow 0} \left( \frac{\partial Z_t(\mathbf{g})}{\partial g_{\sigma,u}} - \frac{\partial Z_t(\mathbf{g})}{\partial g_{\sigma,u}^r} \right). \quad (27)$$

### III. THE KINETIC SK MODEL WITH ASYMMETRIC COUPLINGS

We consider  $N$  interacting elements  $\mathbf{s}_u$  (spins or neurons), taking each element  $i$  at time  $u$  ( $u = 0, \dots, t$ ) a binary state  $s_{i,u} = \{-1, 1\}$ . Interactions take the form of delayed pairwise couplings (i.e.,  $f_n(\mathbf{s}_u, \mathbf{s}_{u-1}) = s_{i,u} s_{j,u-1}$ ). This results in the dynamics of the kinetic Ising model under parallel updates:

$$p(\mathbf{s}_u | \mathbf{s}_{u-1}) = \prod_i \frac{\exp[\beta s_{i,u} h_{i,u}]}{2 \cosh[\beta h_{i,u}]}, \quad (28)$$

$$h_{i,u} = H_{i,u} + \sum_j J_{ij} s_{j,u-1}, \quad (29)$$

where  $\beta$  is the inverse temperature. The system's state at time  $u$  depends on the state of the previous time-step (Fig. 1(a)). Here we use time-dependent fields  $H_{i,u}$  ( $i = 1, \dots, N$ ) whereas couplings  $J_{ij}$  ( $i, j = 1 \dots, N$ ) are constant. However, note that we will assume constant fields for the stationary and steady-state solution.

The generating functional of the model (Eq. 18) is then defined by the functions

$$\epsilon(\mathbf{s}_u | \mathbf{s}_{u-1}) = - \sum_i (\beta s_{i,u} h_{i,u} + \log 2 \cosh[\beta h_{i,u}]), \quad (30)$$

$$\epsilon(\mathbf{s}_{u-1} | \mathbf{s}_u) = - \sum_i (\beta s_{i,u-1} h_{i,u}^r + \log 2 \cosh[\beta h_{i,u}^r]), \quad (31)$$

where  $h_{i,u}^r = H_{i,u} + \sum_j J_{ij} s_{j,u} = h_{i,u+1} + H_{i,u} - H_{i,u+1}$ .

The equilibrium Ising model with random Gaussian symmetric couplings is referred to as the Sherrington-Kirkpatrick (SK) model. In the asymmetric SK model, the couplings  $J_{ij}$  are quenched independent variables, each following a Gaussian distribution

$$p(J_{ij}) = \frac{1}{\sqrt{2\pi\Delta J^2/N}} \exp \left[ -\frac{1}{2\Delta J^2/N} \left( J_{ij} - \frac{J_0}{N} \right)^2 \right], \quad (32)$$

where both the mean  $J_0/N$  and the variance  $\Delta J^2/N$  are proportional to  $1/N$ .

The asymmetric SK system shows a variety of population dynamics when we vary its parameters, e.g., the inverse temperature  $\beta$  and the coupling variance  $\Delta J^2$ . It shows disordered dynamics for large coupling variance both at high and low temperatures (Fig. 1 (b,c)), ordered dynamics for low temperatures and low coupling variance (Fig. 1(e)), and critical dynamics at the phase transition (Fig. 1(d)).

Below, we will assume for simplicity that  $p_0(\mathbf{s}_0) = \delta(\mathbf{s}_0)$  – the initial distribution is a Kronecker delta with one unique value – and ignore the term, but the steps can be generalized to any initial distribution.

### IV. SOLUTION OF THE ASYMMETRIC SHERRINGTON-KIRKPATRICK MODEL

The solution of the kinetic version of the SK model with asymmetric and quenched couplings can be obtained by computing the generating functional averaged over the couplings (known as the configurational average):

$$[Z_t(\mathbf{g})] = \int \prod_{i,j} dJ_{ij} p(J_{ij}) Z_t(\mathbf{g}). \quad (33)$$

This integral cannot be solved directly because of the  $\log 2 \cosh$  terms in Eqs. 30 and 31, which nonlinearly depends on  $J_{ij}$  through  $h_{i,u}$  and  $h_{i,u}^r$ . A path integral method [48] to find a solution is to introduce a delta integral representing  $\beta h_{i,u}$  with an auxiliary variable  $\theta_{i,u} = \beta(H_{i,u} + \sum_j J_{ij} s_{j,u-1})$  as well as  $\beta h_{i,u}^r$  with an auxiliary variable  $\vartheta_{i,u} = \theta_{i,u+1} + \beta(H_{i,u} - H_{i,u+1})$ . Let  $\boldsymbol{\theta} = \{\theta_{i,u}\}$  (note  $u = 1, \dots, t+1$ ) and  $\boldsymbol{\vartheta} = \{\vartheta_{i,u}\}$  ( $u = 0, \dots, t$ ) denote a set of the auxiliary variables. Using conjugate variables  $\hat{\boldsymbol{\theta}} = \{\hat{\theta}_{i,u}\}$  to represent the delta function in the integral form, the configurational average is written as

$$\begin{aligned} [Z_t(\mathbf{g})] = & \frac{1}{(2\pi)^{N(t+1)}} \int d\boldsymbol{\theta} d\hat{\boldsymbol{\theta}} \prod_{i,j} dJ_{ij} p(J_{ij}) \\ & \cdot \sum_{\mathbf{s}_{1:t}} \exp \left[ \sum_{i,u} (s_{i,u} \theta_{i,u} - \log 2 \cosh \theta_{i,u}) \right. \\ & + \sum_{i,u} i \hat{\theta}_{i,u} (\theta_{i,u} - \beta H_{i,u} - \beta \sum_j J_{ij} s_{j,u-1}) \\ & \left. + \Gamma(\mathbf{g}, \mathbf{s}_{0:t}, \boldsymbol{\theta}, \boldsymbol{\vartheta}) \right], \quad (34) \end{aligned}$$

with  $\Gamma(\mathbf{g}, \mathbf{s}_{0:t}, \boldsymbol{\theta}, \boldsymbol{\vartheta}) = \sum_{i,u} \Gamma_{i,u}(\mathbf{g}, \mathbf{s}_{0:t}, \theta_{i,u}, \vartheta_{i,u})$ , where

$$\begin{aligned} \Gamma_{i,u}(\mathbf{g}, \mathbf{s}_{0:t}, \theta_{i,u}, \vartheta_{i,u}) = & g_{i,u} s_{i,u} \\ & + g_{\sigma,u} (s_{i,u} \theta_{i,u} - \log 2 \cosh[\theta_{i,u}]) \\ & + g_{\sigma,u}^r (s_{i,u-1} \vartheta_{i,u} - \log 2 \cosh[\vartheta_{i,u}]). \quad (35) \end{aligned}$$

Note that the summation over  $\hat{\theta}_{i,u}$  is performed over  $u = 1, \dots, t+1$  to retrieve the fields of both the forward and backward trajectories.

Now the integral over  $J_{ij}$  can be performed directly as the integrand only contains linear exponential terms (see a detailed description of the steps in Appendix A). After integrating Eq 34, the configurational average incorporates quadruple-wise interactions between the spins  $\mathbf{s}_{0:t}$  and conjugate variables  $\hat{\boldsymbol{\theta}}$  (Eq. A8), similar to the spin

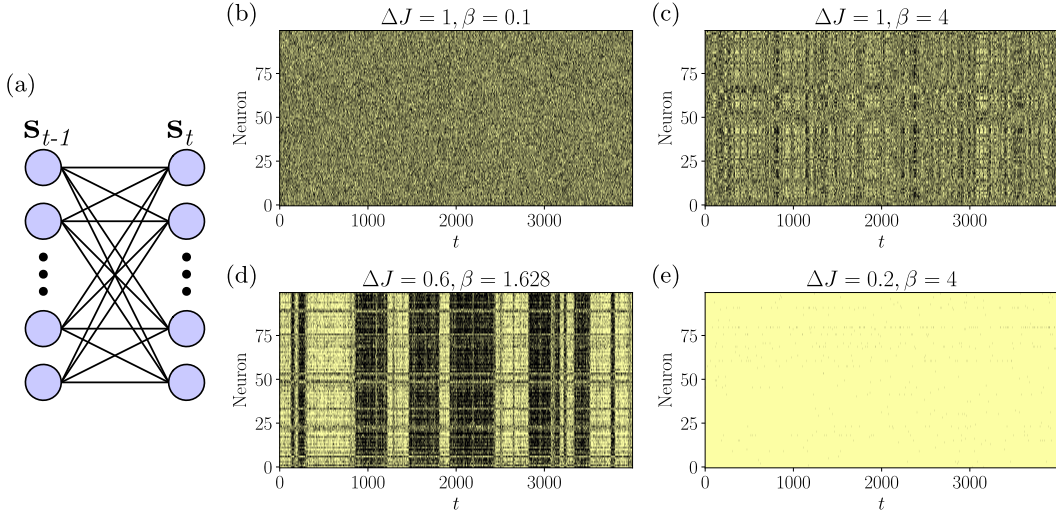


FIG. 1. **Asymmetric kinetic SK model.** (a) The asymmetric kinetic Ising model describes a Markov chain where states at time  $s_u$  depend on pairwise couplings to states  $s_{u-1}$ . (b-e) This model shows disordered dynamics for large coupling variance both at high and low temperatures (b and c), ordered dynamics for low temperatures and low coupling variance (e), and critical dynamics at the phase transition (d).

interactions in the solution of the equilibrium SK model [12]. These higher-order interactions are simplified by introducing Gaussian integrals and a saddle-point approximation in the thermodynamic limit (Eq. A25). By introducing adequate order parameters, the saddle-point solution can be described in terms of the four types of order parameters (Eq. A30). In the case of fully-asymmetric networks, two of these order parameters are found to be zero, yielding a solution in terms of the order parameters  $m_u$  and  $q_{u,v}$  defined by Eqs. 16 and 17 under the configurational average (see Eq. A46). Finally, we show that the conjugate variables  $\hat{\theta}$  in the saddle-point solution can be substituted with an equivalent multivariate Gaussian integral (Eq. A49), leading to a factorized configurational average of the generating functional

$$[Z_t(\mathbf{g})] = \prod_i \sum_{\mathbf{s}_{i,1:t}} \int d\boldsymbol{\xi} p(\boldsymbol{\xi}) \exp \left[ \sum_u s_{i,u} \bar{h}_{i,u}(\xi_u) - \sum_u \log 2 \cosh [\beta \bar{h}_{i,u}(\xi_u)] + \sum_u \Gamma_{i,u}(\mathbf{g}, \mathbf{s}_{0:t}, \beta \bar{h}_{i,u}(\xi_u), \beta \bar{h}_{i,u}^r(\xi_{u+1})) \right], \quad (36)$$

where the stochastic elements  $\boldsymbol{\xi} = (\xi_1, \dots, \xi_{t+1})$  affecting each spin  $i$  follow a multivariate normal distribution  $p(\boldsymbol{\xi}) = \mathcal{N}(\mathbf{0}, \mathbf{q})$ , where the matrix  $\mathbf{q}$  is composed of elements  $q_{u-1,v-1}$  defining the interaction between each pair  $\xi_u, \xi_v$  for  $u, v \in 1, \dots, t+1$ . In this equation, the interactions between spins have been substituted by the same-spin temporal couplings. These self-couplings are

determined by the mean effective fields

$$\bar{h}_{i,u}(\xi_u) = H_{i,u} + J_0 m_{u-1} + \Delta J \xi_u, \quad (37)$$

$$\bar{h}_{i,u}^r(\xi_{u+1}) = H_{i,u} + J_0 m_u + \Delta J \xi_{u+1}, \quad (38)$$

Here the variables  $m_u$  and  $q_{u,v}$  are the order parameters of the system, derived as

$$m_u = \frac{1}{N} \sum_i \int Dz \tanh [\beta \bar{h}_{i,u}(z)], \quad (39)$$

$$q_{u,v} = \frac{1}{N} \sum_i \int Dxy^{(q_{u-1,v-1})} \tanh [\beta \bar{h}_{i,u}(x)] \cdot \tanh [\beta \bar{h}_{i,v}(y)], \quad (40)$$

where the Gaussian stochastic terms are simplified to

$$Dz = \frac{1}{\sqrt{2\pi}} \exp \left[ -\frac{1}{2} z^2 \right], \quad (41)$$

$$Dxy^{(q)} = \frac{1}{2\pi \sqrt{1-q^2}} \exp \left[ -\frac{x^2 + y^2 - 2qxy}{2(1-q^2)} \right]. \quad (42)$$

Note that, in contrast with the equilibrium SK model, magnetizations  $m_u$  are independent of  $q_{u,v}$ . This independence results in the lack of a spin-glass phase suggested by previous studies of the asymmetric SK model [49].

Applying Eqs. 25 and 26 to the configurational average, the conditional entropy results in

$$S_{u|u-1} = - \sum_i \int Dz \left( \beta (H_{i,u} + J_0 m_{u-1}) \tanh [\beta \bar{h}_{i,u}(z)] + \beta^2 \Delta J^2 (1 - \tanh^2 [\beta \bar{h}_{i,u}(z)]) - \log 2 \cosh [\beta \bar{h}_{i,u}(z)] \right), \quad (43)$$

and the reversed conditional entropy in

$$S_{u|u-1}^r = - \sum_i \int Dz \left( \beta (H_{i,u} + J_0 m_u) \tanh [\beta \bar{h}_{i,u-1}(z)] \right. \\ \left. + \beta^2 \Delta J^2 q_{u+1,u-1} (1 - \tanh^2 [\beta \bar{h}_{i,u-1}(z)]) \right. \\ \left. - \log 2 \cosh [\beta \bar{h}_{i,u}^r(z)] \right) \quad (44)$$

Finally using Eq. 27, the entropy production in the steady state simplifies to

$$\sigma_u = \beta^2 \Delta J^2 (1 - q) \sum_i \int Dz (1 - \tanh^2 [\beta \bar{h}_{i,u}(z)]), \quad (45)$$

where we use the steady-state solutions  $m$  and  $q$  of Eqs. 39, 40 for the order parameters in this equation.

## V. RESULTS

### A. Systems without external fields

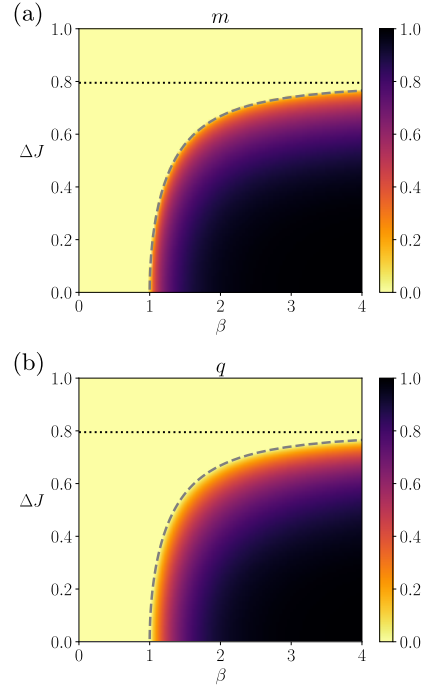
Given the analytical solution of the system, we study the phase space of the SK model. Note that, in contrast with the naive replica-symmetric solution of the equilibrium SK model, the equations above are exact in the model with asymmetric couplings in the thermodynamic limit.

Fig. 2(a) and 2(b) display the phase maps of the steady-state order parameters,  $m$  and  $q$ , derived from Eqs. 39 and 40 as a function of the inverse temperature  $\beta$  and the width of the coupling distribution  $\Delta J$ , when the external fields are fixed at zeros  $H_{i,u} = 0$  and the mean coupling is  $J_0 = 1$ . In this setting, the inverse temperature  $\beta$  controls the magnitude of the couplings. The phase map shows two distinct regions, one in which the order parameters are fixed at zero (zero magnetization and zero self-correlations,  $m = 0$  and  $q = 0$ ) –indicating disordered states– and the other in which the order parameters become positive ( $m > 0$  and  $q > 0$ ) –indicating highly correlated states. Therefore, the system exhibits a nonequilibrium analogue of the paramagnetic-ferromagnetic (disorder-order) phase transition controlled by the parameters,  $\beta$  and  $\Delta J$ . The dashed line in each panel shows the critical values of  $\Delta J$  as a function of  $\beta$ , which is obtained by solving the following equation (see Appendix B),

$$\frac{1}{\beta J_0} = \int Dz (1 - \tanh^2 [\beta (\Delta J z)]) . \quad (46)$$

The solution will be denoted as  $\Delta J^c(\beta)$ .

It should be noted that, depending on the width  $\Delta J$ , the dynamics does or does not undergo the nonequilibrium phase transition by varying the inverse temperature  $\beta$ . The critical  $\Delta J^c(\beta)$  at  $\beta \rightarrow \infty$  is given as  $\Delta J^c(\infty) = 0.79501$  (dotted horizontal line). If the distribution is narrower than the critical value  $J^c(\infty)$ , the



**FIG. 2. Order parameters of the asymmetric SK model with zero fields.** The average magnetization  $m$  and the average delayed self-coupling  $q$  are shown in the phase space of the inverse temperature  $\beta$  and coupling heterogeneity  $\Delta J$  using a model with fixed parameters  $J_0 = 1$ ,  $\Delta H = 0$ . The dashed line represents the critical line separating ordered and disordered phases. The dotted line represents the critical value at zero temperature ( $\beta \rightarrow \infty$ ).

process undergoes the phase transition by changing  $\beta$ . If the distribution is wider than the critical value, the order parameters are fixed at zeros ( $m = 0$ ,  $q = 0$ ) for any  $\beta$ . Note that, at for  $\beta \rightarrow \infty$  (zero temperature), the activation function approaches threshold nonlinearity given by the Heaviside step function; therefore, the process becomes deterministic. That is, for the large values of  $\beta$ , the process approaches deterministic dynamics yielding either ordered or disordered states for smaller or larger  $\Delta J$ , respectively. We remark that the disordered state with  $m = 0$  and  $q = 0$  at the high  $\beta$  (low temperature) does not indicate the spin-glass phase as expected for the equilibrium Ising system (see Appendix C). We confirmed the non-existence of a spin-glass phase by finding that the system decays exponentially in this region (Appendix D).

The reduction in uncertainty at higher  $\beta$  is indicated by the reduction of the conditional entropy (the path entropy)  $S_{u|u-1}$  by increasing  $\beta$  (Fig. 3(a)). This figure additionally shows that the conditional entropy decreases slowly with increasing  $\beta$  along the critical line of the phase transitions. This means that strong couplings and diverse patterns co-exist along the critical line. To the contrary, the time-reversed conditional entropy  $S_{u|u-1}^r$



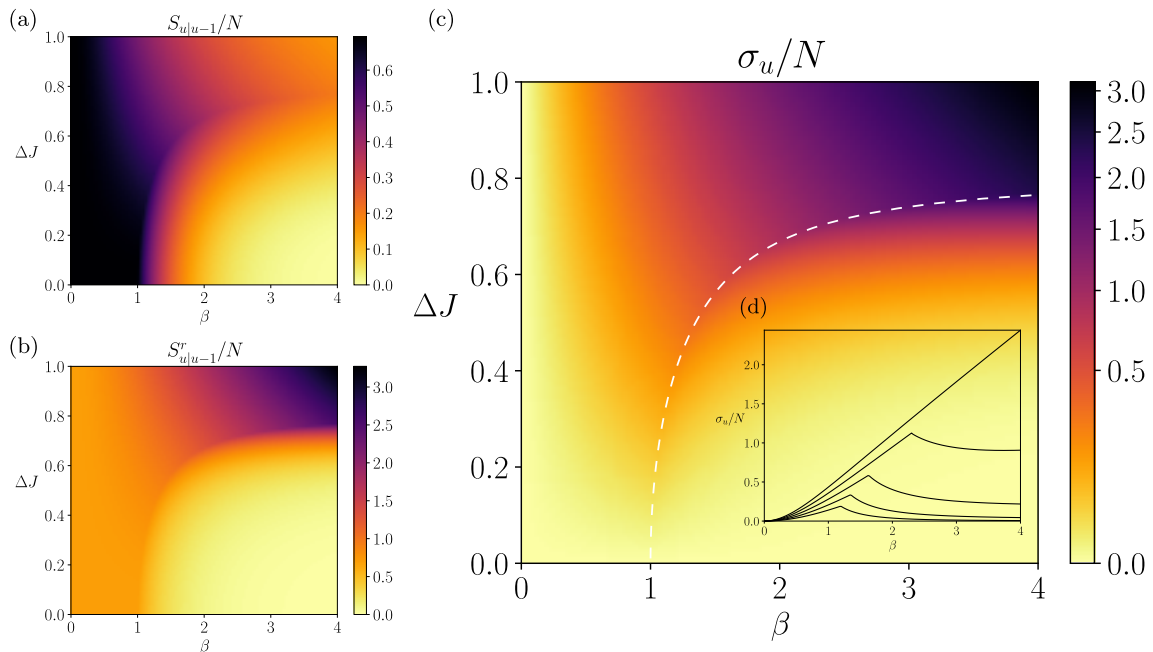


FIG. 3. **Steady-state entropy rate and entropy production of the asymmetric SK model.** (a) The phase space of the conditional entropy  $S_{u|u-1}$  (equivalent to the entropy rate) as a function of the inverse temperature  $\beta$  and the coupling heterogeneity  $\Delta J$ . (b) The conditional entropy of the reverse dynamics  $S^r_{u|u-1}$ . (c) The entropy production at a steady state. The white dashed line is a critical line for the nonequilibrium phase transitions. (d, inset) The horizontal sections of the entropy production ( $\Delta J = 0.4, 0.5, 0.6, 0.7$ , and  $0.7950$ ), showing that it peaks at the critical line. All figures are based on a model with fixed parameters  $H_{i,u} = 0$  and  $J_0 = 1$ .

(Fig. 3(b)) displays opposite characteristics regarding its dependency on  $\beta$  for the broader or narrower coupling distributions. Time-reversed conditional entropy quantifies how surprising the reverse process is under the forward model. With coupling distributions narrower than the critical value  $\Delta J^c(\infty)$ , the time-reversed conditional entropy diminishes by increasing  $\beta$ , indicating that the reverse processes takes place with increasingly high probabilities. This is because the spin state is fixated at all up or down under the ferromagnetic-like state for all time, losing temporal asymmetry. In contrast, the reverse process is less and less likely to happen as the dynamics becomes deterministic by increasing  $\beta$  yet remains disordered, which is realized when the coupling distribution is broader than  $\Delta J^c(\infty)$ . This distinct behaviour between the conditional entropy and its time-reversed version found at the wider coupling distributions and high inverse temperatures yields the strong time-asymmetry in this regime.

The entropy production under the steady-state condition quantifies the difference between the conditional and time-reversed conditional entropy. Fig. 3(c) displays the phase map of the entropy production. The entropy production is maximized at the high  $\beta$  under the broader coupling distributions, where we find a significant difference between these two conditional entropies. Namely, strong time-asymmetry appears when the dynamics are disordered, deterministic processes. Note

that the entropy production increases with  $\beta$  if the coupling distribution is wider than  $\Delta J^c(\infty)$ . In contrast, the entropy production is locally maximized at the critical point (white dashed line) with the narrower coupling distributions than  $\Delta J^c(\infty)$ . For the narrowly distributed couplings, the process exhibits a paramagnetic-like (randomized or disordered) phase at smaller  $\beta$  and a ferromagnetic-like (ordered) phase at higher  $\beta$  (Fig. 2), neither of which can exhibit adequately asymmetric dynamics in time. Time-asymmetry appears between the ordered and disordered phases, namely at the critical point, where the process balances the random and deterministic state transitions. As a consequence, the steady-state entropy production can be a measure of the criticality of this regime (Fig. 3(d)). However, most importantly, the magnitude of the entropy production is far more significant in the regime of large  $\Delta J$  and  $\beta$  than near the critical states.

## B. Systems with uniformly distributed external fields

Next, we apply non-zero external fields to the spins, assuming that the individual fields are sampled from a uniform distribution of the range  $[-\Delta H, \Delta H]$ . Fig. 4(a) and 4(b) shows the  $\beta - \Delta J$  phase map for the order parameters. With this change, we observe non-zero correla-



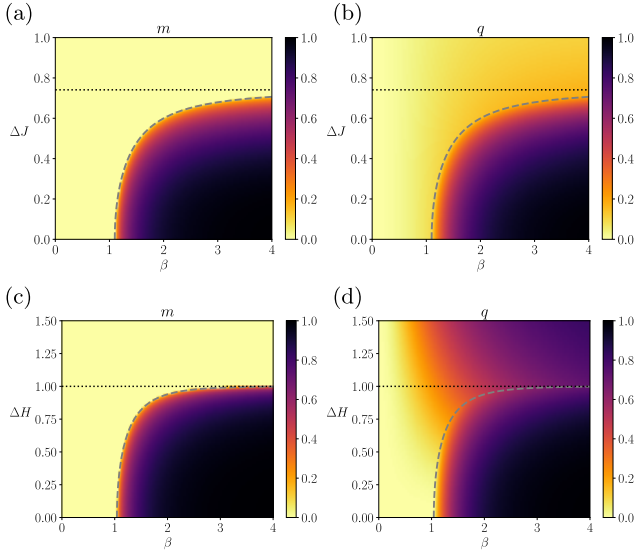


FIG. 4. **Order parameters of the asymmetric SK model with heterogeneous fields.** (a, b) The average magnetization  $m$  and the average delayed self-coupling  $q$  are shown as a function of  $\Delta J$  and  $\beta$ . Fixed parameters are  $J_0 = 1$ ,  $\Delta H = 0.5$ . The dashed line represents the critical line separating ordered and disordered phases. The horizontal dotted line represents the critical  $\Delta J$  at zero temperature ( $\beta \rightarrow \infty$ ). (b, c) The phase maps of order parameters as a function of  $\Delta H$  and  $\beta$ . Fixed parameters are  $J_0 = 1$  and  $\Delta J = 0.2$  and variable. The dashed line is a critical  $\Delta H$  at zero temperature.

tion  $q$  in the area where we previously saw the disordered states ( $m = 0$  and  $q = 0$ , Fig. 2(b)). In contrast, Fig. 4(c) and 4(d) display the order parameters as a function of the inverse temperature and  $\Delta H$ , where we examine the effect of heterogeneity in the external fields while fixing the coupling variability,  $\Delta J = 0.2$ . The critical line of  $\Delta H^c(\beta)$  is obtained in this case as a solution of the following self-consistent equation (Eq. B9):

$$\frac{\Delta H}{J_0} = \int Dz \tanh[\beta(\Delta H + \Delta Jz)]. \quad (47)$$

Since the right-hand side term is less than or equal to 1 regardless of  $\beta$  and  $\Delta J$ , the phase transition occurs only when  $\Delta H < J_0$  is satisfied. Intuitively, there is a competition between dispersion induced by the field diversities  $\Delta H$  and cohesion induced by the mean coupling strength  $J_0$ . The ordered phase takes place only if  $J_0$  counteracts the dispersion tendency by the diverse fields. More precisely, the critical  $\Delta H^c(\beta)$  at the low temperature limit ( $\beta \rightarrow \infty$ ) is obtained by solving  $\Delta H/J_0 = \int Dz \text{sign}[\Delta H + \Delta Jz]$ . Here we have  $\Delta H^c(\infty) = 1$ . We observe the phase transition by varying  $\beta$  if  $\Delta H < \Delta H^c(\infty)$ , and no phase transition if  $\Delta H > \Delta H^c(\infty)$ . Note that  $q$  increases monotonically with  $\beta$  even for  $\Delta H > \Delta H^c(\infty)$  when the distributed fields are introduced.

We now examine the conditional entropy, its reverse, and entropy production for the system with the distributed fields, using the  $\beta$  vs.  $\Delta H$  phase maps. Similarly to the observation in the model without fields, the conditional entropy decreases with higher  $\beta$  (it becomes more deterministic processes, see Fig. 5(a)). The reversed conditional entropy also decreases with increasing  $\beta$  for all  $\Delta H$ , indicating that the reverse process is more and more likely to happen regardless of  $\Delta H$  (Fig. 5(b)). As seen previously, the time-reversed conditional entropy diminishes under the ferromagnetic-like states ( $\Delta H < \Delta H^c(\infty)$ ). In contrast, we also observe the reduction of the reversed conditional entropy at higher  $\beta$  for  $\Delta H > \Delta H^c(\infty)$ . Note that we observed increased correlations  $q$  at higher  $\beta$  for  $\Delta H > \Delta H^c(\infty)$  when we introduced the non-zero external fields (see Fig. 4(d)), which resulted in the reduction of the reversed entropy similarly to the ferromagnetic-like states. Both conditional and reverse conditional entropies decrease much slower along the critical line than in other regions, although with different magnitudes. As a result, we see the maximization of the entropy production around critical points more clearly than the  $\beta$ - $\Delta J$  phase map (Fig. 5(c and 5(d))). Finally, at the zero temperature limit ( $\beta \rightarrow 0$ ), the entropy production peaks at  $\Delta H^c(\infty) = 1$  (Fig. 5(e)).

## VI. DISCUSSION

In this article, we studied in detail the nonequilibrium thermodynamics of the kinetic, asymmetric SK model. As expected, the order parameters reveal that the model exhibits order-disorder nonequilibrium phase transitions analogous to the paramagnetic-ferromagnetic phase transitions in the equilibrium Ising model. There are, however, no dynamics akin to the spin-glass phase (which cannot emerge due to coupling asymmetry). In addition, we show that the steady-state entropy production is maximized near the nonequilibrium phase transition points, being its first derivative discontinuous at the phase transition (Fig. 3(d)). Nevertheless, the entropy production can take even larger values outside the critical regime, especially in disordered systems with low entropy rates, i.e., if the connections are heterogeneous and strong enough to make the dynamics disordered but highly deterministic (Fig. 3(c), top-right). In contrast, the entropy production does not increase when we increase the heterogeneity of external fields (Fig. 5(c)). Our results indicate that a non-smooth change of the steady-state entropy production (or entropy dissipated to an external reservoir) can be a useful indicator of nonequilibrium phase transitions. At the same time, our results suggest that, even if the system shows large entropy production, it does not necessarily indicate the system is near a phase transition. Instead, a combination of the order parameters, entropy rate, and entropy production yields a more precise picture of the complex, disordered systems and their phase

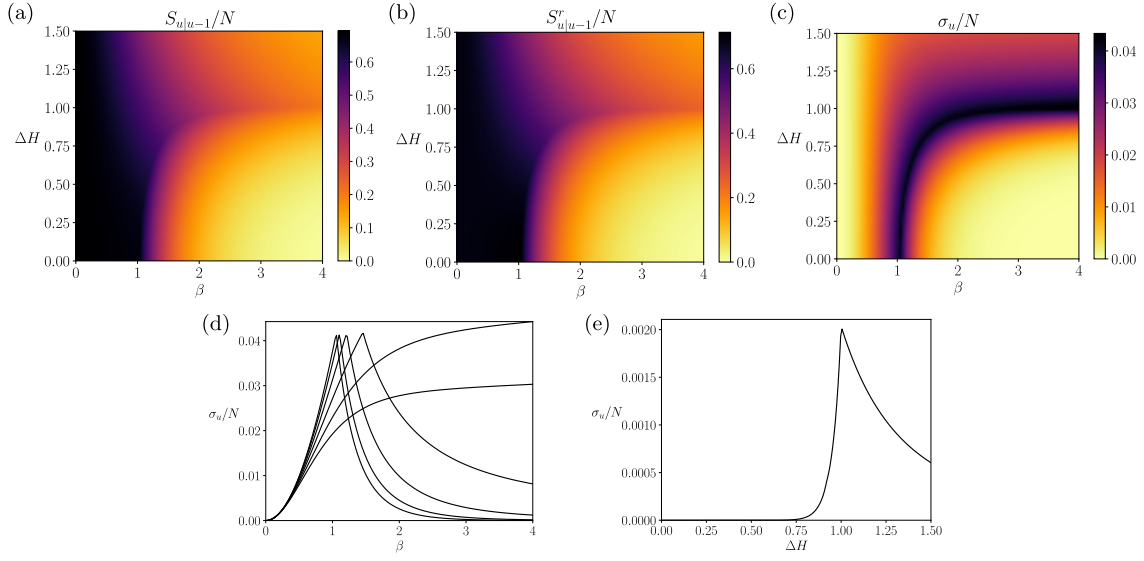


FIG. 5. **Entropy rate and entropy production of the asymmetric SK model with heterogeneous fields.** (a) The normalized conditional entropy  $S_{u|u-1}$  (equivalent to the entropy rate under a steady state). (b) the normalized conditional entropy of the reverse dynamics  $S^r_{u|u-1}$ . (c) The normalized entropy production at a steady state (or the normalized entropy flow). (d) Horizontal sections of the entropy production ( $\Delta H = 0.2, 0.4, 0.6, 0.8, 1.0$ , and  $1.2$ ). It peaks at the critical line. (e) A vertical section of the entropy production at zero temperature ( $\beta \rightarrow \infty$ ). All plots are based on a model with fixed parameters  $J_0 = 1$ , and  $\Delta J = 0.2$  and variable  $\Delta H$  and  $\beta$ .

transitions.

Typically, solutions of the symmetric (equilibrium) SK model involve the replica trick to calculate the configurational average of the logarithm of the partition function [12]. This method involves contradictory assumptions by introducing an integer number of replicas of a system for averaging disorder and then recovering the solution using a continuous number of replicas in the zero limit. This apparent contradiction is not formally resolved, and the method does not always result in the exact solutions, so one must introduce additional assumptions such as replica symmetry-breaking. The path integral method is free from these assumptions, although it can be less flexible than the replica method. For the case of the symmetric SK model, the path integral method does not give a definite analytical solution but needs to be computed with Monte Carlo approaches [50]. Fortunately, as we have shown, the path integral method derives an exact analytical solution for the case of the fully asymmetric nonequilibrium SK model.

Recently, nonequilibrium properties of biological and intelligent systems have received the attention of neuroscience and biological science communities. For example, increased entropy production in macroscopic neural activity was suggested as a signature of physically and cognitively demanding tasks [4], conscious activity [5, 6] or neuropsychiatric diseases like schizophrenia, bipolar disorders, and ADHD [7]. While it is not easy to contrast their findings based on the coarse-grained analysis of ECoG or fMRI data with the present results, our precise characterization of the entropy production of the pro-

totypical system sheds light on what kind of behaviours we might expect from these complicated systems. Most importantly, our results imply two scenarios to increase entropy production by controlling the connection heterogeneity ( $\Delta J$ ) and neuron's nonlinearity ( $\beta$ ). These global changes in the model parameters can be realized in the brain as gain modulation often mediated by neuromodulators [51]. One scenario to increase entropy production is that the system approaches the critical state as seen in the low  $\Delta J$  in Fig. 2 or Fig. 4. The other scenario is to make the system more heterogeneous or sensitive by increasing  $\Delta J$  or  $\beta$ . A significant difference is that the former process maintains stochastic nature while the latter yields deterministic disorder, as indicated by the high or reduced entropy rate. Therefore, the results suggest that it is crucial to investigate the multiple nonequilibrium states to underpin the unconscious (sleep or anesthesia), awake, and engaged states more precisely.

Finally, our analytical solutions offer a benchmark for – the proposed above and other – methods for estimating thermodynamic quantities. For example, characterizing entropy production from brain imaging data requires methods for coarse-graining the phase space [4, 5]. The kinetic SK model can serve as a test bench for such methods as it is an analytically tractable system with a well-known phase space. Moreover, we can use them to examine known and novel mean-field theories in estimating the thermodynamic properties of a large-scale system. For example, one can directly fit the kinetic Ising model to neuronal spiking data by using other types of mean-field methods for finite-size networks [31], from which one can

estimate thermodynamic quantities of the system. Accurate estimation of them in large networks gives closer insights into the nonlinear computations of cortical circuitries. The present exact solutions serve to evaluate these approximation methods applied to large-scale networks, providing a benchmark of the thermodynamics quantities in an infinitely large network.

## ACKNOWLEDGMENTS

MA was funded by the European Union's Horizon 2020 research and innovation programme under the Marie Skłodowska-Curie grant agreement No 892715. HS is supported by JSPS KAKENHI Grant Number JP 20K11709, 21H05246, and New Energy and Industrial Technology Development Organization (NEDO), Japan.

## CONTRIBUTIONS

M.A. and H.S. designed and reviewed research; M.A. contributed the analytical results. M.A. and M.I. contributed the numerical results; M.A., M.I., and H.S. contributed the theoretical review and wrote the paper.

- 
- [1] N. Wiener, Newtonian and Bergsonian time, in *Cybernetics, or control and communication in the animal and the machine*, 2nd ed (John Wiley & Sons Inc, Hoboken, NJ, US, 1961) pp. 30–44.
  - [2] D. Kondepudi and I. Prigogine, *Modern thermodynamics: from heat engines to dissipative structures* (John Wiley & Sons, 2014).
  - [3] J. L. England, Statistical physics of self-replication, *The Journal of chemical physics* **139**, 09B623-1 (2013).
  - [4] C. W. Lynn, E. J. Cornblath, L. Papadopoulos, M. A. Bertolero, and D. S. Bassett, Broken detailed balance and entropy production in the human brain, *Proceedings of the National Academy of Sciences* **118** (2021).
  - [5] Y. S. Perl, H. Bocaccio, C. Pallavicini, I. Pérez-Ipiña, S. Laureys, H. Laufs, M. Kringelbach, G. Deco, and E. Tagliazucchi, Nonequilibrium brain dynamics as a signature of consciousness, *Physical Review E* **104**, 014411 (2021).
  - [6] L. A. de la Fuente, F. Zamberlan, H. Bocaccio, M. Kringelbach, G. Deco, Y. S. Perl, C. Pallavicini, and E. Tagliazucchi, Temporal irreversibility of neural dynamics as a signature of consciousness, *Cerebral Cortex* 10.1093/cercor/bhac177 (2022).
  - [7] G. Deco, Y. S. Perl, J. D. Sitt, E. Tagliazucchi, and M. L. Kringelbach, Deep learning the arrow of time in brain activity: Characterising brain-environment behavioural interactions in health and disease, *bioRxiv* (2021).
  - [8] U. Seifert, Stochastic thermodynamics, fluctuation theorems and molecular machines, *Reports on progress in physics* **75**, 126001 (2012).
  - [9] T. Herpich, J. Thingna, and M. Esposito, Collective power: minimal model for thermodynamics of nonequilibrium phase transitions, *Physical Review X* **8**, 031056 (2018).
  - [10] M. Suñé and A. Imparato, Out-of-equilibrium clock model at the verge of criticality, *Physical Review Letters* **123**, 070601 (2019).
  - [11] T. Herpich, T. Cossetto, G. Falasco, and M. Esposito, Stochastic thermodynamics of all-to-all interacting many-body systems, *New Journal of Physics* **22**, 063005 (2020).
  - [12] H. Nishimori, *Statistical physics of spin glasses and information processing: an introduction* (Clarendon Press, 2001).
  - [13] Y. Roudi, B. Dunn, and J. Hertz, Multi-neuronal activity and functional connectivity in cell assemblies, *Current opinion in neurobiology* **32**, 38 (2015).
  - [14] A. H. Lang, H. Li, J. J. Collins, and P. Mehta, Epigenetic landscapes explain partially reprogrammed cells and identify key reprogramming genes, *PLoS computational biology* **10**, e1003734 (2014).
  - [15] D. Sherrington and S. Kirkpatrick, Solvable model of a spin-glass, *Physical review letters* **35**, 1792 (1975).
  - [16] G. Parisi, A sequence of approximated solutions to the sk model for spin glasses, *Journal of Physics A: Mathematical and General* **13**, L115 (1980).
  - [17] R. Brunetti, G. Parisi, and F. Ritort, Asymmetric Little spin-glass model, *Physical Review B* **46**, 5339 (1992).
  - [18] J. Schnakenberg, Network theory of microscopic and macroscopic behavior of master equation systems, *Reviews of Modern Physics* **48**, 571 (1976).
  - [19] P. Gaspard, Time-reversed dynamical entropy and irreversibility in markovian random processes, *Journal of statistical physics* **117**, 599 (2004).
  - [20] S. Ito, M. Oizumi, and S.-i. Amari, Unified framework for the entropy production and the stochastic interaction based on information geometry, *Physical Review Research* **2**, 033048 (2020).
  - [21] C. Jarzynski, Hamiltonian Derivation of a Detailed Fluctuation Theorem, *Journal of Statistical Physics* **98**, 77 (2000).
  - [22] C. Maes, Local detailed balance, *SciPost Physics Lecture Notes* , 032 (2021).
  - [23] T. Hatano and S.-i. Sasa, Steady-state thermodynamics of langevin systems, *Physical review letters* **86**, 3463 (2001).
  - [24] A. Dechant, S.-i. Sasa, and S. Ito, Geometric decomposition of entropy production in out-of-equilibrium systems, *Physical Review Research* **4**, L012034 (2022).
  - [25] R. Cofré and C. Maldonado, Information entropy production of maximum entropy markov chains from spike trains, *Entropy* **20**, 10.3390/e20010034 (2018).

- [26] R. Cofré, L. Videla, and F. Rosas, An Introduction to the Non-Equilibrium Steady States of Maximum Entropy Spike Trains, *Entropy* **21**, 884 (2019).
- [27] A. Crisanti and H. Sompolinsky, Path integral approach to random neural networks, *Physical Review E* **98**, 062120 (2018).
- [28] Y. Zhang and A. C. Barato, Critical behavior of entropy production and learning rate: Ising model with an oscillating field, *Journal of Statistical Mechanics: Theory and Experiment* **2016**, 113207 (2016).
- [29] C. E. F. Noa, P. E. Harunari, M. J. de Oliveira, and C. E. Fiore, Entropy production as a tool for characterizing nonequilibrium phase transitions, *Physical Review E* **100**, 012104 (2019).
- [30] L. Crochik and T. Tomé, Entropy production in the majority-vote model, *Physical Review E* **72**, 057103 (2005).
- [31] M. Aguilera, S. A. Moosavi, and H. Shimazaki, A unifying framework for mean-field theories of asymmetric kinetic ising systems, *Nature communications* **12**, 1 (2021).
- [32] E. T. Jaynes, *Probability theory: The logic of science* (Cambridge university press, 2003).
- [33] E. T. Jaynes, Macroscopic prediction, in *Complex Systems—Operational Approaches in Neurobiology, Physics, and Computers* (Springer, 1985) pp. 254–269.
- [34] S. Pressé, K. Ghosh, J. Lee, and K. A. Dill, Principles of maximum entropy and maximum caliber in statistical physics, *Reviews of Modern Physics* **85**, 1115 (2013).
- [35] H. Ge, S. Pressé, K. Ghosh, and K. A. Dill, Markov processes follow from the principle of maximum caliber, *The Journal of chemical physics* **136**, 064108 (2012).
- [36] A. K. Livesey and J. Skilling, Maximum entropy theory, *Acta Crystallographica Section A: Foundations of Crystallography* **41**, 113 (1985).
- [37] A. Kolmogoroff, *Grundbegriffe der Wahrscheinlichkeitsrechnung*, Vol. 2 (Springer-Verlag, 2013).
- [38] E. D. Schneider and J. J. Kay, Life as a manifestation of the second law of thermodynamics, *Mathematical and computer modelling* **19**, 25 (1994).
- [39] C. Van den Broeck and M. Esposito, Ensemble and trajectory thermodynamics: A brief introduction, *Physica A: Statistical Mechanics and its Applications* **418**, 6 (2015).
- [40] G. E. Crooks, Nonequilibrium measurements of free energy differences for microscopically reversible markovian systems, *Journal of Statistical Physics* **90**, 1481 (1998).
- [41] M. Esposito and C. Van den Broeck, Three detailed fluctuation theorems, *Physical review letters* **104**, 090601 (2010).
- [42] M. Igarashi, Entropy production for discrete-time markov processes, *arXiv*, 2205.07214 (2022).
- [43] Y.-J. Yang and H. Qian, Unified formalism for entropy production and fluctuation relations, *Physical Review E* **101**, 022129 (2020).
- [44] H. Touchette, The large deviation approach to statistical mechanics, *Physics Reports* **478**, 1 (2009).
- [45] H. Touchette and R. J. Harris, Large deviation approach to nonequilibrium systems, in *Nonequilibrium Statistical Physics of Small Systems* (John Wiley & Sons, Ltd, 2013) Chap. 11, pp. 335–360.
- [46] H. Touchette, Introduction to dynamical large deviations of markov processes, *Physica A: Statistical Mechanics and its Applications* **504**, 5 (2018).
- [47] V. Lecomte, C. Appert-Rolland, and F. van Wijland, Thermodynamic Formalism for Systems with Markov Dynamics, *Journal of Statistical Physics* **127**, 51 (2007).
- [48] J. A. Hertz, Y. Roudi, and P. Sollich, Path integral methods for the dynamics of stochastic and disordered systems, *Journal of Physics A: Mathematical and Theoretical* **50**, 033001 (2016).
- [49] A. Crisanti and H. Sompolinsky, Dynamics of spin systems with randomly asymmetric bonds: Ising spins and glauher dynamics, *Physical Review A* **37**, 4865 (1988).
- [50] H. Eissfeller and M. Opper, Mean-field monte carlo approach to the sherrington-kirkpatrick model with asymmetric couplings, *Physical Review E* **50**, 709 (1994).
- [51] E. Eldar, J. D. Cohen, and Y. Niv, The effects of neural gain on attention and learning, *Nature neuroscience* **16**, 1146 (2013).
- [52] P. Joy, P. A. Kumar, and S. Date, The relationship between field-cooled and zero-field-cooled susceptibilities of some ordered magnetic systems, *Journal of physics: condensed matter* **10**, 11049 (1998).
- [53] L. Cugliandolo, J. Kurchan, and F. Ritort, Evidence of aging in spin-glass mean-field models, *Physical Review B* **49**, 6331 (1994).
- [54] H. Sompolinsky and A. Zippelius, Dynamic theory of the spin-glass phase, *Physical Review Letters* **47**, 359 (1981).

# Nonequilibrium thermodynamics of the asymmetric Sherrington-Kirkpatrick model: Supplementary Information

Miguel Aguilera  
*School of Engineering and Informatics  
University of Sussex  
Falmer, Brighton. United Kingdom*

Masanao Igarashi  
*Department of Applied Physics,  
Graduate School of Engineering, Hokkaido University  
Sapporo, Japan*

Hideaki Shimazaki  
*Center for Human Nature, Artificial Intelligence,  
and Neuroscience (CHAIN), Hokkaido University  
Sapporo, Japan*

## Appendix A: A path integral approach to asymmetric SK systems

In this appendix, we compute the generating functional of the asymmetric kinetic Ising model averaged over the quenched couplings with Gaussian distributions, known as the configurational average.

The probability density of a specific trajectory of the kinetic Ising model,  $\mathbf{s}_{0:t} = \{\mathbf{s}_0, \mathbf{s}_1, \dots, \mathbf{s}_t\}$ , is defined as

$$\begin{aligned} p(\mathbf{s}_{0:t}) &= \prod_{u=1}^t p(\mathbf{s}_u | \mathbf{s}_{u-1}) p(\mathbf{s}_0) \\ &= \exp \left[ \beta \sum_{i,u} s_{i,u} h_{i,u} - \sum_{i,u} \log 2 \cosh [\beta h_{i,u}] \right] p(\mathbf{s}_0), \end{aligned} \quad (\text{A1})$$

where

$$h_{i,u} = H_{i,u} + \sum_j J_{ij} s_{j,u-1}. \quad (\text{A2})$$

Here the summation over  $u$  is taken for  $u = 1, \dots, t$ . For simplicity, we will assume that  $p(\mathbf{s}_0)$  only contains one possible value, that is, the initial distribution is a Kronecker delta  $\delta(\mathbf{s}_0)$ . Although this allows us to ignore the term, the next steps are generalizable to any initial distributions.

In equilibrium systems, the partition function provides the statistical moments of the equilibrium distribution. Here, to find the above statistical properties expected from ensemble trajectories of the asymmetric SK model (Eqs. 14, 15 in the main text) as well as its steady-state entropy production (Eq. 11), we introduce the following generating functional or dynamical partition function:

$$\begin{aligned} Z_t(\mathbf{g}) &= \sum_{\mathbf{s}_{0:t}} p(\mathbf{s}_{0:t}) \exp \left[ \sum_{i,u} g_{i,u} s_{i,u} \right. \\ &\quad \left. + \sum_{i,u} g_{\sigma,u} (\beta s_{i,u} h_{i,u} - \log 2 \cosh [\beta h_{i,u}]) + \sum_{i,u} g_{\sigma,u}^r (\beta s_{i,u-1} h_{i,u}^r - \log 2 \cosh [\beta h_{i,u}^r]) \right] \\ &= \sum_{\mathbf{s}_{0:t}} \exp \left[ \sum_{i,u} s_{i,u} \beta h_{i,u} - \log 2 \cosh [\beta h_{i,u}] + \sum_{i,u} g_{i,u} s_{i,u} \right. \\ &\quad \left. + \sum_{i,u} g_{\sigma,u} (s_{i,u} \beta h_{i,u} - \log 2 \cosh [\beta h_{i,u}]) + \sum_{i,u} g_{\sigma,u}^r (s_{i,u-1} \beta h_{i,u}^r - \log 2 \cosh [\beta h_{i,u}^r]) \right], \end{aligned} \quad (\text{A3})$$

where  $h_{i,u}^r = H_{i,u} + \sum_j J_{ij} s_{j,u} = h_{i,u+1} + H_{i,u} - H_{i,u+1}$ . Note that  $h_{i,u}$  have to be defined up to  $t+1$  to recover the backwards trajectory. The terms  $g_{i,u}$  are designed to obtain the moments and other statistics of the system and  $g_{\sigma,u}, g_{\sigma,u}^r$  its conditional and reversed conditional entropy terms at time  $u$ .

The configurational average over Gaussian couplings (Eq. 32) of the generating functional is computed as

$$[Z_t(\mathbf{g})] = \int \prod_{i,j} dJ_{ij} p(J_{ij}) Z_t(\mathbf{g}). \quad (\text{A4})$$

The configurational average can be solved using the following path integral method. To obtain the path integral form, we first insert an appropriate delta integral for the effective fields of each unit for the time steps  $u = 1, \dots, t+1$  to the above equation:

$$\begin{aligned} 1 &= \int d\boldsymbol{\theta} \prod_{i,u} \delta(\theta_{i,u} - \beta h_{i,u}) \\ &= \frac{1}{(2\pi)^{N(t+1)}} \int d\boldsymbol{\theta} d\hat{\boldsymbol{\theta}} \exp \left[ \sum_{i,u} i\hat{\theta}_{i,u} (\theta_{i,u} - \beta H_{i,u} - \beta \sum_j J_{ij} s_{j,u-1}) \right], \end{aligned} \quad (\text{A5})$$

where  $\boldsymbol{\theta}$  is the  $N(t+1)$ -dimensional vector composed of the effective fields  $\theta_{i,u}$  ( $i = 1, \dots, N$  and  $u = 1, \dots, t+1$ ).  $\hat{\boldsymbol{\theta}}$  is the  $N(t+1)$ -dimensional conjugate effective field, and we used  $\delta(x-a) = \frac{1}{2\pi} \int_{-\infty}^{\infty} e^{i\zeta(x-a)} d\zeta$ . Note that, from now on, all summations and products involving the conjugate effective field  $\hat{\boldsymbol{\theta}}$  (as well as the order parameters we introduce later) will be performed over the range  $u = 1, \dots, t+1$ . Next, we replace  $\beta h_{i,u}$  in Eq. A3 with the auxiliary variable  $\theta_{i,u}$  as well as  $\beta h_{i,u}^r$  of the reversed couplings at time  $u$  with an auxiliary variable  $\vartheta_{i,u} = \theta_{i,u+1} + \beta(H_{i,u} - H_{i,u+1})$ , and place them inside the integral with respect to  $\boldsymbol{\theta}$  (i.e., we perform the operation,  $f(a) = \int f(x)\delta(x-a)dx$ ). The configurational average is written as

$$\begin{aligned} [Z_t(\mathbf{g})] &= \frac{1}{(2\pi)^{N(t+1)}} \int d\boldsymbol{\theta} d\hat{\boldsymbol{\theta}} \prod_{i,j} dJ_{ij} p(J_{ij}) \\ &\cdot \sum_{\mathbf{s}_{1:t}} \exp \left[ \sum_{i,u} s_{i,u} (g_{i,u} + \theta_{i,u}) - \log 2 \cosh \theta_{i,u} + \sum_{i,u} g_{\sigma,u} (s_{i,u} \theta_{i,u} - \sum_{i,u} \log 2 \cosh \theta_{i,u}) \right. \\ &\left. + \sum_{i,u} g_{\sigma,u}^r (s_{i,u-1} \vartheta_{i,u} - \log 2 \cosh \vartheta_{i,u}) + \sum_{i,u} i\hat{\theta}_{i,u} (\theta_{i,u} - \beta H_{i,u} - \beta \sum_j J_{ij} s_{j,u-1}) \right]. \end{aligned} \quad (\text{A6})$$

Using the Gaussian integral formula  $\int dx \frac{1}{\sqrt{2\pi b}} \exp \left[ ax - \frac{(x-c)^2}{2b} \right] = \exp \left[ ac + \frac{a^2}{2} b \right]$ , the expectation of  $\exp[aJ_{ij}]$  is computed as

$$\int dJ_{ij} p(J_{ij}) \exp[aJ_{ij}] = \exp \left[ aJ_0/N + \frac{a^2}{2} J_{\sigma}^2/N \right]. \quad (\text{A7})$$

Hence the integral related to  $J_{ij}$  in Eq. A6 is computed as

$$\begin{aligned} &\int \left[ \prod_{i,j} dJ_{ij} p(J_{ij}) \right] \exp \left[ - \sum_{i,u} i\hat{\theta}_{i,u} \beta \sum_j J_{ij} s_{j,u-1} \right] \\ &= \prod_{i,j} \left[ \int dJ_{ij} p(J_{ij}) \exp \left[ - \beta \left( \sum_u i\hat{\theta}_{i,u} s_{j,u-1} \right) J_{ij} \right] \right] \\ &= \prod_{i,j} \exp \left[ - \beta \left( \sum_u i\hat{\theta}_{i,u} s_{j,u-1} \right) \frac{J_0}{N} + \beta^2 \left( \sum_u i\hat{\theta}_{i,u} s_{j,u-1} \right)^2 \frac{J_{\sigma}^2}{2N} \right] \\ &= \prod_{i,j} \exp \left[ - \frac{\beta J_0}{N} \sum_u i\hat{\theta}_{i,u} s_{j,u-1} + \frac{\beta^2 \Delta J^2}{2N} \sum_{u,v} i\hat{\theta}_{i,u} s_{j,u-1} i\hat{\theta}_{i,v} s_{j,v-1} \right]. \end{aligned} \quad (\text{A8})$$

Using this result, the Gaussian integral form of the partition function is given as

$$\begin{aligned}
[Z_t(\mathbf{g})] = & \frac{1}{(2\pi)^{N(t+1)}} \int d\boldsymbol{\theta} d\hat{\boldsymbol{\theta}} \sum_{\mathbf{s}_{1:t}} \exp \left[ \sum_{i,u} s_{i,u} (g_{i,u} + \theta_{i,u}) - \sum_{i,u} \log 2 \cosh \theta_{i,u} \right. \\
& + \sum_{i,u} g_{\sigma,u} (s_{i,u} \theta_{i,u} - \log 2 \cosh \theta_{i,u}) + \sum_{i,u} g_{\sigma,u}^r (s_{i,u-1} \vartheta_{i,u} - \log 2 \cosh \vartheta_{i,u}) \\
& + \sum_{i,u} i \hat{\theta}_{i,u} (\theta_{i,u} - \beta H_{i,u}) - \sum_u N \beta J_0 \left( \frac{1}{N} \sum_i i \hat{\theta}_{i,u} \right) \left( \frac{1}{N} \sum_j s_{j,u-1} \right) \\
& \left. + \frac{\beta^2 \Delta J^2}{2N} \sum_{i,u} \left( i \hat{\theta}_{i,u} \right)^2 + \sum_{u>v} N \beta^2 \Delta J^2 \left( \frac{1}{N} \sum_i i \hat{\theta}_{i,u} i \hat{\theta}_{i,v} \right) \left( \frac{1}{N} \sum_j s_{j,u-1} s_{j,v-1} \right) \right]. \quad (\text{A9})
\end{aligned}$$

Note that, for the term of summation over  $u, v$ , we separated the  $u = v$  terms from the rest, resulting in elimination of the spin variables because  $s_{j,u-1} s_{j,u-1} = 1$ .

### 1. Gaussian integral and saddle node approximation

We want to evaluate the expression above with the Gaussian integral by the saddle node approximation, and show that the saddle node solutions that will become order parameters. For this goal, we first give an outline of the derivation, and then apply the steps to the above equation.

Let  $C$  be a real value, and  $x$  and  $y$  be complex values. Eq. A9) contains the term in the form of  $\exp[Cxy]$ . We can represent this term by a double Gaussian integral (a pair of the Gaussian integral formulas) with the form:

$$\begin{aligned}
\exp[Cxy] &= \exp \left[ \frac{C}{2} \left( \frac{1}{2}(x+y)^2 + \frac{1}{2}(i(x-y))^2 \right) \right] \\
&= \frac{C}{4\pi} \int dz_R dz_I \exp \left[ \frac{C}{2} \left\{ -\frac{1}{2}z_R^2 - \frac{1}{2}z_I^2 + (x+y)z_R + i(x-y)z_I \right\} \right] \\
&= \frac{C}{4\pi} \int dz_R dz_I \exp \left[ \frac{C}{2} \left\{ -\frac{1}{2}z_R^2 - \frac{1}{2}z_I^2 + x(z_R + iz_I) + y(z_R - iz_I) \right\} \right], \quad (\text{A10})
\end{aligned}$$

Because the integrand is an analytic function, we can change the contour of the path integral in the complex space so that it includes the saddle point solution. This contour integration produces the original value,  $\exp[Cxy]$ . Therefore,  $z_R$  and  $z_I$  are no longer real values but can be complex values.

When  $x$  and  $y$  are random variables, we can approximate the expectation of  $\exp[Cxy]$  by the saddle node solutions when the constant  $C$  is large:

$$\int p(x, y) \exp[Cxy] dx dy \approx \exp \left[ \frac{C}{2} \left\{ -\frac{1}{2}z_R^{*2} - \frac{1}{2}z_I^{*2} + \log \int p(x, y) \exp[x(z_R^* + iz_I^*) + y(z_R^* - iz_I^*)] dx dy \right\} \right], \quad (\text{A11})$$

where  $z_R^*$  and  $z_I^*$  are the saddle point solutions that extremize the contents of the brackets  $\{\}$  in Eq. A10. The solutions are given by

$$z_R^* = \langle x + y \rangle, \quad (\text{A12})$$

$$z_I^* = i \langle x - y \rangle, \quad (\text{A13})$$

where the bracket  $\langle \cdot \rangle$  represents

$$\langle f(x, y) \rangle = \frac{\int p(x, y) \exp[x(z_R^* + iz_I^*) + y(z_R^* - iz_I^*)] f(x, y) dx dy}{\int p(x, y) \exp[x(z_R^* + iz_I^*) + y(z_R^* - iz_I^*)] dx dy} \quad (\text{A14})$$

We remind that for the saddle-point solution  $z_I^*$  is derived from substituting the exponent by its Taylor expansion around the minimum, i.e.,  $f(z_I) = f(z_I^*) + \frac{1}{2}f''(z_I^*)(z_I - i(x-y))^2 + \mathcal{O}((z_I - i(x-y))^3)$ , which in this case has an imaginary value.

In order to obtain a more intuitive saddle point solution, we can perform a change of variables

$$z_1^* = \frac{1}{2}(z_R^* + iz_I^*), \quad z_2 = \frac{1}{2}(z_R^* - iz_I^*) \quad (\text{A15})$$

$$z_R^* = z_1^* + z_2^*, \quad z_I^* = i(z_1^* - z_2^*), \quad (\text{A16})$$



resulting in

$$\int p(x, y) \exp[Cxy] dx dy \approx \exp \left[ \frac{C}{2} \left\{ -z_1^* z_2^* + \log \int p(x, y) \exp[xz_1^* + yz_2^*] \right\} \right], \quad (\text{A17})$$

and

$$z_1^* = \langle y \rangle \quad (\text{A18})$$

$$z_2^* = \langle x \rangle \quad (\text{A19})$$

In a nutshell, the process described above consists of 1) introducing a pair of Gaussian integrals, 2) finding a saddle point solution, and 3) performing a change of variable to recover a solution in terms of expectations of the original variables. We now repeat the process for the integral of the partition function.

**(i) Gaussian integrals.** First we introduce Gaussian integrals by applying Eq. A10 to the quadratic terms in the partition function. Using  $C = N\beta J_0$ ,  $x_{u-1} = \frac{1}{N} \sum_j s_{j,u-1}$  and  $y_u = -\frac{1}{N} \sum_i i\hat{\theta}_{i,u}$ , we obtain

$$\begin{aligned} & \exp \left[ \sum_u (-N\beta J_0) \left( \frac{1}{N} \sum_i i\hat{\theta}_{i,u} \right) \left( \frac{1}{N} \sum_j s_{j,u-1} \right) \right] \\ &= \prod_u \exp[Cx_{u-1}y_u] \\ &= \left( \frac{C}{4\pi} \right)^t \int \prod_u dM_u^+ dM_u^- \exp \left[ \frac{C}{2} \left( -\frac{1}{2}(M_u^+)^2 - \frac{1}{2}(M_u^-)^2 + x_{u-1}(M_u^+ + iM_u^-) + y_u(M_u^+ - iM_u^-) \right) \right], \quad (\text{A20}) \end{aligned}$$

where  $M_u^+$  and  $M_u^-$  are real-valued integral variables. Similarly, using  $C = \frac{1}{2}N\beta^2\Delta J^2$ ,  $x_{u-1,v-1} = \frac{1}{N} \sum_j s_{j,u-1}s_{j,v-1}$ ,  $y_{u,v} = \frac{1}{N} \sum_i \hat{\theta}_{i,u}\hat{\theta}_{i,v}$ , we have

$$\begin{aligned} & \exp \left[ \sum_{u,v} N \frac{\beta^2 \Delta J^2}{2} \left( \frac{1}{N} \sum_i i\hat{\theta}_{i,u} i\hat{\theta}_{i,v} \right) \left( \frac{1}{N} \sum_j s_{j,u-1} s_{j,v-1} \right) \right] \\ &= \prod_{u,v} \exp[Cx_{u-1,v-1}y_{u,v}] \\ &= \left( \frac{C}{4\pi} \right)^{2t} \int \prod_{u,v} dQ_{u,v}^+ dQ_{u,v}^- \exp \left[ \frac{C}{2} \left( -\frac{1}{2}(Q_{u,v}^+)^2 - \frac{1}{2}(Q_{u,v}^-)^2 + x_{u-1,v-1}(Q_{u,v}^+ + iQ_{u,v}^-) + y_{u,v}(Q_{u,v}^+ - iQ_{u,v}^-) \right) \right], \quad (\text{A21}) \end{aligned}$$

where  $Q_{u,v}^+$  and  $Q_{u,v}^-$  are real values. Note that the products over  $u$  and  $v$  are performed over the range  $1, \dots, t+1$ .

With these double Gaussian integrals and defining  $d\mathbf{M} = \prod_u dM_u^+ dM_u^-$  and  $d\mathbf{Q} = \prod_{u,v} dQ_{u,v}^+ dQ_{u,v}^-$  we can rewrite the partition function as

$$\begin{aligned} [Z_t(\mathbf{g})] &= \frac{(N\beta J_0)^t (N\beta^2 \Delta J^2)^{2t}}{(4\pi)^{3t}} \int d\mathbf{M} d\mathbf{Q} \exp \left[ -N\beta J_0 \sum_u \frac{(M_u^+)^2 + (M_u^-)^2}{4} \right. \\ &\quad \left. - N\beta^2 \Delta J^2 \sum_{u>v} \frac{(Q_{u,v}^+)^2 + (Q_{u,v}^-)^2}{4} + \log \sum_{\mathbf{s}_{1:t}} \int d\boldsymbol{\theta} d\hat{\boldsymbol{\theta}} e^{\Phi(\mathbf{s}_{0:t}, \boldsymbol{\theta}) + \Omega(\hat{\boldsymbol{\theta}}, \boldsymbol{\theta})} \right], \quad (\text{A22}) \end{aligned}$$

where the rest of the terms related to the random variable  $\mathbf{s}$  and  $\boldsymbol{\theta}, \hat{\boldsymbol{\theta}}$  from the Gaussian integral can be separated

into the terms

$$\begin{aligned}\Phi(\mathbf{s}_{0:t}, \boldsymbol{\theta}) &= \sum_{i,u} (g_{i,u} + \theta_{i,u}) s_{i,u} - \sum_{i,u} \log 2 \cosh [\theta_{i,u}] \\ &\quad + \sum_{i,u} g_{\sigma,u} (s_{i,u} \theta_{i,u} - \log 2 \cosh \theta_{i,u}) + \sum_{i,u} g_{\sigma,u}^r (s_{i,u-1} \vartheta_{i,u} - \log 2 \cosh \vartheta_{i,u}) \\ &\quad + \sum_{i,u} \beta J_0 \frac{M_u^+ + i M_u^-}{2} s_{i,u-1} + \sum_{i,u>v} \beta^2 \Delta J^2 \frac{Q_{u,v}^+ + i Q_{u,v}^-}{2} s_{i,u-1} s_{i,v-1}\end{aligned}\quad (\text{A23})$$

$$\begin{aligned}\Omega(\hat{\boldsymbol{\theta}}, \boldsymbol{\theta}) &= \sum_{i,u} (\theta_{i,u} - \beta H_{i,u} - \beta J_0 \frac{M_u^+ - i M_u^-}{2}) i \hat{\theta}_{i,u} \\ &\quad + \frac{\beta^2 \Delta J^2}{2} \sum_{i,u} (i \hat{\theta}_{i,u})^2 + \beta^2 \Delta J^2 \sum_{i,u>v} \frac{Q_{u,v}^+ - i Q_{u,v}^-}{2} i \hat{\theta}_{i,u} i \hat{\theta}_{i,v} - N(t+1) \log 2\pi.\end{aligned}\quad (\text{A24})$$

Now, the next two steps for solving the integral is to find a saddle point solution, and then perform a change of variables. In the next section, we find that the solutions result in the order parameters of the system.

**(ii) Saddle point integral solution.** The exponent of the above integrand is proportional to  $N$ , making it possible to evaluate the integral by steepest descent, giving the saddle-point solution as

$$\begin{aligned}[Z_t(\mathbf{g})] &= \exp \left[ \left\{ -N\beta J_0 \sum_u \frac{(M_u^+)^2 + (M_u^-)^2}{4} - N\beta^2 \Delta J^2 \sum_{u>v} \frac{(Q_{u,v}^+)^2 + (Q_{u,v}^-)^2}{4} \right. \right. \\ &\quad \left. \left. + \log \sum_{\mathbf{s}_{1:t}} \int d\boldsymbol{\theta} d\hat{\boldsymbol{\theta}} e^{\Phi(\mathbf{s}_{0:t}, \boldsymbol{\theta}) + \Omega(\hat{\boldsymbol{\theta}}, \boldsymbol{\theta})} \right\} \right]\end{aligned}\quad (\text{A25})$$

where the values of  $\mathbf{M}, \mathbf{Q}$  are chosen to extremize (maximize or minimize) the quantity between the braces  $\{\}$ . As in the solution in Eqs. A12 and A13, the solutions  $(M_u^+)^*, (Q_{u,v}^+)^*$  and  $(M_u^-)^*, (Q_{u,v}^-)^*$  are combinations of the average statistics of the variables of interest (multiplied by the imaginary unit in the case of the latter).

**(iii) Change of the variables.** Having order parameters in this form can be cumbersome. We simplify them to directly capture the average statistics of the system by performing a change of variables at the saddle-point solution as exemplified in Eq. A15, resulting in:

$$\mu_u = \frac{M_u^+ + i M_u^-}{2}, \quad m_{u-1} = \frac{M_u^+ - i M_u^-}{2} \quad (\text{A26})$$

$$\rho_{u,v} = \frac{Q_{u,v}^+ + i Q_{u,v}^-}{2}, \quad q_{u-1,v-1} = \frac{Q_{u,v}^+ - i Q_{u,v}^-}{2} \quad (\text{A27})$$

or equivalently

$$M_u^+ = m_{u-1} + \mu_u \quad M_u^- = i(m_{u-1} - \mu_u), \quad (\text{A28})$$

$$Q_{u,v}^+ = q_{u-1,v-1} + \rho_{u,v}, \quad Q_{u,v}^- = i(q_{u-1,v-1} - \rho_{u,v}), \quad (\text{A29})$$

where now we expect all  $\mathbf{m}, \boldsymbol{\mu}, \mathbf{q}, \boldsymbol{\rho}$  to be real-valued.

This results in

$$\begin{aligned}[Z_t(\mathbf{g})] &= \exp \left[ \left\{ -N\beta J_0 \sum_u \mu_u m_{u-1} - N\beta^2 \Delta J^2 \sum_{u>v} \rho_{u,v} q_{u-1,v-1} \right. \right. \\ &\quad \left. \left. + \log \sum_{\mathbf{s}_{1:t}} \int d\boldsymbol{\theta} d\hat{\boldsymbol{\theta}} e^{\Phi(\mathbf{s}_{0:t}, \boldsymbol{\theta}) + \Omega(\hat{\boldsymbol{\theta}}, \boldsymbol{\theta})} \right\} \right],\end{aligned}\quad (\text{A30})$$

where now  $\mathbf{m}, \boldsymbol{\mu}, \mathbf{q}, \boldsymbol{\rho}$  are chosen to extremize the quantity between the braces. Also we define the terms

$$\begin{aligned} \Phi(\mathbf{s}_{0:t}, \boldsymbol{\theta}) = & \sum_{i,u} (g_{i,u} + \theta_{i,u}) s_{i,u} - \sum_{i,u} \log 2 \cosh [\theta_{i,u}] + \sum_{i,u} g_{\sigma,u} (s_{i,u} \theta_{i,u} - \log 2 \cosh \theta_{i,u}) \\ & + \sum_{i,u} g_{\sigma,u}^r (s_{i,u-1} \vartheta_{i,u} - \log 2 \cosh \vartheta_{i,u}) + \sum_{i,u} \beta J_0 \mu_u s_{i,u-1} + \sum_{i,u>v} \beta^2 \Delta J^2 \rho_{u,v} s_{i,u-1} s_{i,v-1} \end{aligned} \quad (\text{A31})$$

$$\begin{aligned} \Omega(\hat{\boldsymbol{\theta}}, \boldsymbol{\theta}) = & \sum_{i,u} (\theta_{i,u} - \beta H_{i,u} - \beta J_0 m_{u-1}) i \hat{\theta}_{i,u} \\ & + \frac{\beta^2 \Delta J^2}{2} \sum_{i,u} (i \hat{\theta}_{i,u})^2 + \beta^2 \Delta J^2 \sum_{i,u>v} q_{u-1,v-1} i \hat{\theta}_{i,u} i \hat{\theta}_{i,v} - N(t+1) \log 2\pi. \end{aligned} \quad (\text{A32})$$

Note that the summation of  $u$  or  $v$  related to the order parameters are performed over the range  $1, \dots, t+1$ . Also notice that integration over disordered connections has removed coupling between units and replaced it with same-unit temporal couplings  $\boldsymbol{\rho}$  and varying effective fields, which are also independent between units, resulting in a mean-field solution where the activity of different spins is independent.

In the next section, we specify the conditions of the extrema, from which we find that some of the extrema are the order parameters.

## 2. Introduction of the order parameters

The configurational average of the generating functional holds relations similar to Eqs. 21, 22:

$$\lim_{\mathbf{g} \rightarrow \mathbf{0}} \frac{\partial [Z_t(\mathbf{g})]}{\partial g_{i,u}} = [\langle s_{i,u} \rangle], \quad (\text{A33})$$

$$\lim_{\mathbf{g} \rightarrow \mathbf{0}} \frac{\partial^2 [Z_t(\mathbf{g})]}{\partial g_{i,u} \partial g_{j,v}} = [\langle s_{i,u} s_{j,v} \rangle]. \quad (\text{A34})$$

In addition, we have the following identities that will be helpful in eliminating spurious solutions

$$\lim_{\mathbf{g} \rightarrow \mathbf{0}} \frac{\partial Z_t(\mathbf{g})}{\partial H_{i,u}} = \beta (m_{i,u} - m_{i,u}) = 0, \quad (\text{A35})$$

$$\lim_{\mathbf{g} \rightarrow \mathbf{0}} \frac{\partial^2 Z_t(\mathbf{g})}{\partial H_{i,u} \partial H_{j,v}} = \beta \left( \frac{\partial m_{i,u}}{\partial H_{j,v}} - \frac{\partial m_{i,v}}{\partial H_{j,v}} \right) = 0. \quad (\text{A36})$$

To derive the order parameters, we calculate the same partial derivatives using Eq. A30. Given the equations above while taking into account that  $\lim_{\mathbf{g} \rightarrow \mathbf{0}} [Z_t(\mathbf{g})] = 1$ , we can compute the order parameters of the system as

$$\begin{aligned} \lim_{\mathbf{g} \rightarrow \mathbf{0}} \frac{\partial [Z_t(\mathbf{g})]}{\partial g_{i,u}} = & \lim_{\mathbf{g} \rightarrow \mathbf{0}} \frac{\sum_{\mathbf{s}_{1:t}} \int d\boldsymbol{\theta} d\hat{\boldsymbol{\theta}} s_{i,u} e^{\Phi(\mathbf{s}_{0:t}, \boldsymbol{\theta}) + \Omega(\hat{\boldsymbol{\theta}}, \boldsymbol{\theta})}}{\sum_{\mathbf{s}_{1:t}} \int d\boldsymbol{\theta} d\hat{\boldsymbol{\theta}} e^{\Phi(\mathbf{s}_{0:t}, \boldsymbol{\theta}) + \Omega(\hat{\boldsymbol{\theta}}, \boldsymbol{\theta})}} [Z_t(\mathbf{g})] \\ = & \langle s_{i,u} \rangle_* = [\langle s_{i,u} \rangle], \end{aligned} \quad (\text{A37})$$

$$\begin{aligned} \lim_{\mathbf{g} \rightarrow \mathbf{0}} \frac{\partial^2 [Z_t(\mathbf{g})]}{\partial g_{i,u} \partial g_{j,v}} = & \lim_{\mathbf{g} \rightarrow \mathbf{0}} \frac{\sum_{\mathbf{s}_{1:t}} \int d\boldsymbol{\theta} d\hat{\boldsymbol{\theta}} s_{i,u} s_{j,v} e^{\Phi(\mathbf{s}_{0:t}, \boldsymbol{\theta}) + \Omega(\hat{\boldsymbol{\theta}}, \boldsymbol{\theta})}}{\sum_{\mathbf{s}_{1:t}} \int d\boldsymbol{\theta} d\hat{\boldsymbol{\theta}} e^{\Phi(\mathbf{s}_{0:t}, \boldsymbol{\theta}) + \Omega(\hat{\boldsymbol{\theta}}, \boldsymbol{\theta})}} [Z_t(\mathbf{g})] \\ = & \langle s_{i,u} s_{j,v} \rangle_* = [\langle s_{i,u} s_{j,v} \rangle], \end{aligned} \quad (\text{A38})$$

$$\begin{aligned} \lim_{\mathbf{g} \rightarrow \mathbf{0}} \frac{\partial [Z_t(\mathbf{g})]}{\partial H_{i,u}} = & \lim_{\mathbf{g} \rightarrow \mathbf{0}} \frac{\sum_{\mathbf{s}_{1:t}} \int d\boldsymbol{\theta} d\hat{\boldsymbol{\theta}} \beta i \hat{\theta}_{i,u} e^{\Phi(\mathbf{s}_{0:t}, \boldsymbol{\theta}) + \Omega(\hat{\boldsymbol{\theta}}, \boldsymbol{\theta})}}{\sum_{\mathbf{s}_{1:t}} \int d\boldsymbol{\theta} d\hat{\boldsymbol{\theta}} e^{\Phi(\mathbf{s}_{0:t}, \boldsymbol{\theta}) + \Omega(\hat{\boldsymbol{\theta}}, \boldsymbol{\theta})}} [Z_t(\mathbf{g})] \\ = & -\beta \langle i \hat{\theta}_{i,u} \rangle_* = 0, \end{aligned} \quad (\text{A39})$$

$$\begin{aligned} \lim_{\mathbf{g} \rightarrow \mathbf{0}} \frac{\partial^2 [Z_t(\mathbf{g})]}{\partial H_{i,u} \partial H_{j,v}} = & \lim_{\mathbf{g} \rightarrow \mathbf{0}} \frac{\sum_{\mathbf{s}_{1:t}} \int d\boldsymbol{\theta} d\hat{\boldsymbol{\theta}} \beta^2 i \hat{\theta}_{i,u} i \hat{\theta}_{j,v} e^{\Phi(\mathbf{s}_{0:t}, \boldsymbol{\theta}) + \Omega(\hat{\boldsymbol{\theta}}, \boldsymbol{\theta})}}{\sum_{\mathbf{s}_{1:t}} \int d\boldsymbol{\theta} d\hat{\boldsymbol{\theta}} e^{\Phi(\mathbf{s}_{0:t}, \boldsymbol{\theta}) + \Omega(\hat{\boldsymbol{\theta}}, \boldsymbol{\theta})}} [Z_t(\mathbf{g})] \\ = & \beta^2 \langle i \hat{\theta}_{i,u} i \hat{\theta}_{i,v} \rangle_* = 0, \end{aligned} \quad (\text{A40})$$

where we define

$$\left\langle f(\mathbf{s}_{0:t}, \hat{\boldsymbol{\theta}}) \right\rangle_* = \frac{\sum_{\mathbf{s}_{1:t}} \int d\boldsymbol{\theta} d\hat{\boldsymbol{\theta}} f(\mathbf{s}_{0:t}, \hat{\boldsymbol{\theta}}) e^{\Phi(\mathbf{s}_{0:t}, \boldsymbol{\theta}) + \Omega(\hat{\boldsymbol{\theta}}, \boldsymbol{\theta})}}{\sum_{\mathbf{s}_{1:t}} \int d\boldsymbol{\theta} d\hat{\boldsymbol{\theta}} e^{\Phi(\mathbf{s}_{0:t}, \boldsymbol{\theta}) + \Omega(\hat{\boldsymbol{\theta}}, \boldsymbol{\theta})}}. \quad (\text{A41})$$

Here we should note that, as there is no coupling between units, for  $i \neq j$  we have a factorized solution  $[\langle s_{i,u} s_{j,v} \rangle] = \langle s_{i,u} s_{j,v} \rangle_* = \langle s_{i,u} \rangle_* \langle s_{j,v} \rangle_*$ .

To obtain the values of the order parameters, we extremize the contents of the braces, finding

$$\lim_{\mathbf{g} \rightarrow \mathbf{0}} \frac{\partial \log[Z_t(\mathbf{g})]}{\partial \mu_{u+1}} = \beta J_0 \left( \sum_i \langle s_{i,u} \rangle_* - N m_u \right) = 0; \quad m_u^* = \frac{1}{N} \sum_i [\langle s_{i,u} \rangle]. \quad (\text{A42})$$

$$\lim_{\mathbf{g} \rightarrow \mathbf{0}} \frac{\partial \log[Z_t(\mathbf{g})]}{\partial m_{u-1}} = -\beta J_0 \left( \sum_i \langle i \hat{\theta}_{i,u} \rangle_* + N \mu_u \right) = 0; \quad \mu_u^* = 0. \quad (\text{A43})$$

$$\lim_{\mathbf{g} \rightarrow \mathbf{0}} \frac{\partial \log[Z_t(\mathbf{g})]}{\partial \rho_{u+1,v+1}} = N \beta^2 \Delta J^2 \left( \sum_i \langle s_{i,u} s_{i,v} \rangle_* - N q_{u,v} \right) = 0; \quad q_{u,v}^* = \frac{1}{N} \sum_i [\langle s_{i,u} s_{i,v} \rangle]. \quad (\text{A44})$$

$$\lim_{\mathbf{g} \rightarrow \mathbf{0}} \frac{\partial \log[Z_t(\mathbf{g})]}{\partial q_{u-1,v-1}} = N \beta^2 \Delta J^2 \left( \sum_i \langle i \hat{\theta}_{i,u} i \hat{\theta}_{i,v} \rangle_* - N \rho_{u,v} \right) = 0; \quad \rho_{u,v}^* = 0. \quad (\text{A45})$$

Here,  $\mathbf{m}^*, \boldsymbol{\mu}^*, \mathbf{q}^*, \boldsymbol{\rho}^*$  provide the saddle-point solution of the configurational average integral. This is equivalent to finding the saddle-point solutions  $\mathbf{M}^*, \mathbf{Q}^*$  above. In the next sections, we study this solution. For simplicity, we will remove the  $*$  exponents from the saddle point solutions.

### 3. Mean-field solutions

After solving the saddle-point integral, we have the following generating functional

$$[Z_t(\mathbf{g})] = \sum_{\mathbf{s}_{1:t}} \int d\boldsymbol{\theta} d\hat{\boldsymbol{\theta}} e^{\Phi(\mathbf{s}_{0:t}, \boldsymbol{\theta}) + \Omega(\hat{\boldsymbol{\theta}}, \boldsymbol{\theta})} \quad (\text{A46})$$

At this point, we want to remove the effective fields  $\boldsymbol{\theta}$  and effective conjugate fields  $\hat{\boldsymbol{\theta}}$ . For this goal, (i) we first remove the effective conjugate fields  $\hat{\boldsymbol{\theta}}$  by recovering delta functions from their integral forms. Then, (ii) we revert the effective fields  $\boldsymbol{\theta}$  by removing the delta function. This results in the mean-field (factorized) generating functional, from which we obtain the mean-field solutions of order parameters, conditional entropy, or entropy production.

**(i) Removing effective conjugate fields** We first remove the conjugate fields by recovering a delta function. We rewrite

$$e^{\Omega(\hat{\boldsymbol{\theta}}, \boldsymbol{\theta})} = \prod_i \frac{1}{(2\pi)^{N(t+1)}} \exp \left[ \sum_u (\theta_{i,u} - \beta H_{i,u} - \beta J_0 m_{u-1}) i \hat{\theta}_{i,u} + \frac{\beta^2 \Delta J^2}{2} \sum_{uv} q_{u-1,v-1} i \hat{\theta}_{i,u} i \hat{\theta}_{i,v} \right] \quad (\text{A47})$$

defining  $q_{u-1,u-1} = 1$  and  $q_{u-1,v-1} = q_{v-1,u-1}$  to define a symmetric matrix. Note that the saddle-node solution Eq. A44 is defined only for  $u > v$ .

We can remove the quadratic terms of  $\hat{\boldsymbol{\theta}}$  by applying  $N(t+1)$ -dimensional multivariate Gaussian integrals of the form

$$e^{-\frac{1}{2} \sum_{uv} K_{u,v} x_u x_v} = \frac{1}{\sqrt{(2\pi)^t |K^{-1}|}} \int d\mathbf{z} e^{-\frac{1}{2} \sum_{uv} K_{u,v} z_u z_v - \sum_{uv} K_{u,v} i x_u z_v} \quad (\text{A48})$$

for  $x_u = \beta \Delta J \hat{\theta}_{i,u}$  and  $K_{u,v} = q_{u-1,v-1}$ . Applying this Gaussian integral transformation to an exponent with negative sign is formally known as a Hubbard–Stratonovich transformation. Similarly, we can remove the quadratic terms of

$\hat{\vartheta}$  by applying  $N$  univariate Gaussian integrals, obtaining

$$\begin{aligned} \int d\hat{\boldsymbol{\theta}} e^{\Omega(\hat{\boldsymbol{\theta}}, \boldsymbol{\theta})} &= \frac{1}{(2\pi)^{N(t+1)}} \prod_i \int d\hat{\boldsymbol{\theta}} dz p(\mathbf{z}) \\ &\cdot \exp \left[ \sum_u i\hat{\theta}_{i,u} (\theta_{i,u} - \beta H_{i,u} - \beta J_0 m_{u-1}) - \beta \Delta J \sum_{uv} q_{u-1,v-1} i\hat{\theta}_{i,u} z_v \right] \\ &= \prod_i \int dz p(\mathbf{z}) \prod_u \delta \left( \theta_{i,u} - \beta \bar{h}_{i,u}(\mathbf{z}) \right), \end{aligned} \quad (\text{A49})$$

where  $\mathbf{z} = (z_1, \dots, z_{t+1})$ , and the distribution  $p(\mathbf{z}) = \mathcal{N}(0, \boldsymbol{\Sigma})$  is a multivariate Gaussian with zero mean and inverse covariance  $\boldsymbol{\Sigma}^{-1} = \mathbf{q}$ , and

$$\bar{h}_{i,u}(\mathbf{z}) = H_{i,u} + J_0 m_{u-1} + \Delta J \sum_v z_v q_{u-1,v-1}, \quad (\text{A50})$$

We can simplify the expressions above into

$$\bar{h}_{i,u}(\xi_u) = H_{i,u} + J_0 m_{u-1} + \Delta J \xi_u \quad (\text{A51})$$

with  $\xi_u = \sum_v z_v q_{u-1,v-1}$ . Let  $\boldsymbol{\xi} = (\xi_1, \dots, \xi_{t+1})$ , then it follows  $p(\boldsymbol{\xi}) = \mathcal{N}(0, \mathbf{q})$ . Similarly we can derive

$$\bar{h}_{i,u}^r(\xi_{u+1}) = H_{i,u} + J_0 m_u + \Delta J \xi_{u+1} \quad (\text{A52})$$

**(ii) Removing effective fields** We now revert the effective fields  $\boldsymbol{\theta}$  to  $\beta \bar{h}_{i,u}(\mathbf{z})$  by removing the delta function, which replaces the original  $\beta h_{i,u}$  with the mean-field equivalent.

Introducing the equivalences in the previous section, we have

$$\begin{aligned} e^{\Phi(\mathbf{s}_{0:t}, \boldsymbol{\theta})} &= \prod_i \exp \left[ \sum_u s_{i,u} (g_{i,u} + \theta_{i,u}) - \sum_u \log 2 \cosh [\theta_{i,u}] \right. \\ &\quad \left. + \sum_u g_{\sigma,u} (s_{i,u} \theta_{i,u} - \log 2 \cosh \theta_{i,u}) + \sum_u g_{\sigma,u}^r (s_{i,u-1} \vartheta_{i,u} - \log 2 \cosh \vartheta_{i,u}) \right] \end{aligned} \quad (\text{A53})$$

which leads us to the mean-field solution of the configurational average of the generating functional

$$\begin{aligned} [Z_t(\mathbf{g})] &= \int d\boldsymbol{\theta} \sum_{\mathbf{s}_{1:t}} e^{\Phi(\mathbf{s}_{0:t}, \boldsymbol{\theta})} \prod_i \int d\boldsymbol{\xi} p(\boldsymbol{\xi}) \prod_u \delta \left( \theta_{i,u} - \beta \bar{h}_{i,u}(\xi_u) \right) \\ &= \prod_i \sum_{\mathbf{s}_{1:t}} \int d\boldsymbol{\xi} p(\boldsymbol{\xi}) \exp \left[ \sum_u s_{i,u} (g_{i,u} + \beta \bar{h}_{i,u}(\xi_u)) - \sum_u \log 2 \cosh [\beta \bar{h}_{i,u}(\xi_u)] \right. \\ &\quad \left. + \sum_u \beta (g_{\sigma,u} s_{i,u} \bar{h}_{i,u}(\xi_u) + g_{\sigma,u}^r s_{i,u-1} \bar{h}_{i,u}^r(\xi_{u+1})) \right. \\ &\quad \left. - \sum_u (g_{\sigma,u} \log 2 \cosh [\beta \bar{h}_{i,u}(\xi_u)] - g_{\sigma,u}^r \log 2 \cosh [\beta \bar{h}_{i,u}^r(\xi_{u+1})]) \right], \end{aligned} \quad (\text{A54})$$

where the summation over  $u$  is taken for the range from 1 to  $t$ . With  $\boldsymbol{\xi}$  defined in the range  $u = 1, \dots, t+1$ , we can recover the values of  $\bar{h}_{i,u}$  and  $\bar{h}_{i,u}^r$  for all time steps.

From this equation, we can derive the mean magnetization and the equal-time correlation of the  $i$ th unit. We note that the diagonal of the covariance matrix of  $\boldsymbol{\xi}$  is equal to 1, hence we arrive at

$$m_{i,u} = \lim_{\mathbf{g} \rightarrow \mathbf{0}} \frac{\partial [Z_t(\mathbf{g})]}{\partial g_{i,u}} = \int D\mathbf{z} \tanh [\beta \bar{h}_{i,u}(z)], \quad (\text{A55})$$

$$R_{ii,uv} = \lim_{\mathbf{g} \rightarrow \mathbf{0}} \frac{\partial^2 [Z_t(\mathbf{g})]}{\partial g_{i,u} \partial g_{j,v}} = \int D\mathbf{x} y^{(q_{u-1,v-1})} \tanh [\beta \bar{h}_{i,u}(x)] \tanh [\beta \bar{h}_{i,v}(y)], \quad (\text{A56})$$

where

$$Dz = \frac{1}{\sqrt{2\pi}} e^{-\frac{1}{2}z^2} \quad (\text{A57})$$

$$Dxy^{(q)} = \frac{1}{2\pi\sqrt{1-q^2}} e^{-\frac{x^2+y^2-2qxy}{2(1-q^2)}} \quad (\text{A58})$$

The resulting equations look similar to the symmetric SK model, but the order parameter  $\mathbf{q}$  does not affect the computation of  $m_u$ .

We obtain order parameters

$$m_u = \frac{1}{N} \sum_i m_{i,u} = \frac{1}{N} \sum_i \int Dz \tanh [\beta (H_{i,u} + J_0 m_{u-1} + \Delta J z)], \quad (\text{A59})$$

$$q_{u,v} = \frac{1}{N} \sum_i R_{ii,uv} = \frac{1}{N} \sum_i \int Dxy(q_{u-1,v-1}) \tanh [\beta (H_{i,u} + J_0 m_{u-1} + \Delta J x)] \tanh [\beta (H_{i,u} + J_0 m_{u-1} + \Delta J \xi_u)]. \quad (\text{A60})$$

Note that magnetizations  $m_u$  are independent of  $q_{u,v}$ . This is consistent with findings of the asymmetric SK model lacking a spin-glass phase [49].

The conditional entropy results in

$$\begin{aligned} S_{u|u-1} &= - \lim_{\mathbf{g} \rightarrow \mathbf{0}} \frac{\partial [Z_t(\mathbf{g})]}{\partial g_{\sigma,u}} = \sum_i \int p(\boldsymbol{\xi}) \left( \tanh [\beta \bar{h}_{i,u}(\xi_u)] \beta \bar{h}_{i,u}(\xi_u) - \log 2 \cosh [\beta \bar{h}_{i,u}(\xi_u)] \right) \\ &= - \sum_i \int p(\boldsymbol{\xi}) \left( \tanh [\beta (H_{i,u} + J_0 m_{u-1} + \Delta J \xi_u)] \beta (H_{i,u} + J_0 m_{u-1} + \Delta J \xi_u) \right. \\ &\quad \left. - \log 2 \cosh [\beta (H_{i,u} + J_0 m_{u-1} + \Delta J \xi_u)] \right) \\ &= - \sum_i \int Dz \left( \beta (H_{i,u} + J_0 m_{u-1}) \tanh [\beta (H_{i,u} + J_0 m_{u-1} + \Delta J z)] \right. \\ &\quad \left. + \beta^2 \Delta J^2 (1 - \tanh^2 [\beta (H_{i,u} + J_0 m_{u-1} + \Delta J z)]) \right. \\ &\quad \left. - \log 2 \cosh [\beta (H_{i,u} + J_0 m_{u-1} + \Delta J z)] \right). \end{aligned} \quad (\text{A61})$$

Similarly, the reversed conditional entropy results in

$$\begin{aligned} S_{u|u-1}^r &= - \lim_{\mathbf{g} \rightarrow \mathbf{0}} \frac{\partial [Z_t(\mathbf{g})]}{\partial g_{\sigma,u}} = \sum_i \int p(\boldsymbol{\xi}) \left( \tanh [\beta \bar{h}_{i,u-1}(\xi_u)] \beta \bar{h}_{i,u}^r(\xi_{u+1}) - \log 2 \cosh \beta \bar{h}_{i,u}^r(\xi_{u+1}) \right) \\ &= - \sum_i \int p(\boldsymbol{\xi}) \left( \tanh [\beta \bar{h}_{i,u-1}(\xi_{u-1})] (\beta (H_{i,u} + J_0 m_u + \Delta J \xi_{u+1})) \right. \\ &\quad \left. - \log 2 \cosh [\beta (H_{i,u} + J_0 m_u + \Delta J \xi_{u+1})] \right) \\ &= - \sum_i \int Dz \left( (\beta H_{i,u} + \beta J_0 m_{u+1}) \tanh [\beta (H_{i,u-1} + J_0 m_{u-2} + \Delta J z)] \right. \\ &\quad \left. + \beta^2 \Delta J^2 q_{u+1,u-1} (1 - \tanh^2 [\beta (H_{i,u-1} + J_0 m_{u-2} + \Delta J z)]) \right. \\ &\quad \left. - \log 2 \cosh [\beta (H_{i,u} + J_0 m_{u+1} + \Delta J z)] \right). \end{aligned} \quad (\text{A62})$$

where  $\xi_{u+1}$  is decomposed as a conditional Gaussian distribution for a given  $\xi_{u-1}$  as  $\xi_{u+1} = q_{u+1,u-1} \xi_{u-1} + \sqrt{1 - q_{u+1,u-1}^2} \zeta_{u+1}$  where  $\zeta_{u+1}$  is a normalized Gaussian independent of  $\xi_{u-1}$  and the term  $q_{u+1,u-1}$  the covariance between variables.

Note that in the steady state in which we have  $m_u = m_{u-1} = m$ , the entropy production simplifies to

$$\sigma_u = S_{u|u-1} - S_{u|u-1}^r = \beta^2 \Delta J^2 (1 - q) \sum_i \int Dz (1 - \tanh^2 [\beta (H_i + J_0 m + \Delta J z)]) \quad (\text{A63})$$

where  $m$  and  $q$  are the steady-state solutions of Eqs. A59, A60.

## Appendix B: Ferromagnetic critical phase transition in the infinite kinetic Ising model with Gaussian couplings and uniform weights

We define a kinetic Ising network of infinite size, with random external fields  $H_{i,u} = H_i$ , where  $H_i$  are uniformly distributed following  $\mathcal{U}(-\Delta H, \Delta H)$ , and couplings  $J_{ij}$  follow a Gaussian distribution  $\mathcal{N}(\frac{1}{N}, \frac{\Delta J^2}{N})$ .

As we have found that the asymmetric SK model with arbitrary fields follows a mean-field solution, calculating the effects of disorder in the fields becomes easier, as we can approximate the update equations of the order parameters in the thermodynamic limit  $N \rightarrow \infty$  as an integral with a large number of units:

$$\begin{aligned} m_u &= \frac{1}{N} \sum_i m_{i,u} = \frac{1}{2\Delta H} \int_{-\Delta H}^{\Delta H} dh \int Dz \tanh[\beta(h + J_0 m_{u-1} + \Delta Jz)] \\ &= \frac{1}{2\beta\Delta H} \int Dz \log \frac{\cosh[\beta(\Delta H + J_0 m_{u-1} + \Delta Jz)]}{\cosh[\beta(-\Delta H + J_0 m_{u-1} + \Delta Jz)]}. \end{aligned} \quad (\text{B1})$$

Similarly, the delayed self-correlation parameter:

$$\begin{aligned} q_{u,v} &= \frac{1}{N} \sum_i R_{ii,u,v} = \frac{1}{2\Delta H} \int_{-\Delta H}^{\Delta H} dh \int Dxy(q_{u-1,v-1}) \tanh[\beta(h + J_0 m_{u-1} + \Delta Jx)] \tanh[\beta(h + J_0 m_{v-1} + \Delta Jy)] \\ &= 1 + \frac{1}{2\beta\Delta H} \int Dxy(q_{u-1,v-1}) \frac{(e^{2\beta H_{v,y}} - e^{2\beta H_{u,x}})}{(e^{2\beta H_{v,y}} + e^{2\beta H_{u,x}})} \log \left[ \frac{e^{-2\beta\Delta H} + e^{2\beta H_{u,x}}}{e^{2\beta\Delta H} + e^{2\beta H_{u,x}}} \frac{e^{2\beta\Delta H} + e^{2\beta H_{v,y}}}{e^{-2\beta\Delta H} + e^{2\beta H_{v,y}}} \right], \end{aligned} \quad (\text{B2})$$

with  $H_{u,x} = J_0 m_{u-1} + \Delta Jx$  and  $H_{v,y} = J_0 m_{v-1} + \Delta Jy$ .

In the zero-temperature case,  $\beta \rightarrow \infty$ , these expressions have the following limits:

$$m_u = \frac{1}{2\beta\Delta H} \int Dz (|\Delta H + J_0 m_{u-1} + \Delta Jz| - |-\Delta H + J_0 m_{u-1} + \Delta Jz|), \quad (\text{B3})$$

$$q_{u,v} = 1 + \frac{1}{2\beta\Delta H} \int Dxy(q_{u-1,v-1}) \text{sign}[H_{v,y} - H_{u,x}] \beta \left( |\Delta H + H_{u,x}| - |\Delta H - H_{u,x}| - |\Delta H + H_{v,y}| + |\Delta H - H_{v,y}| \right). \quad (\text{B4})$$

Finally, the normalized conditional entropy in the thermodynamic limit and normalized reversed conditional entropy are given as

$$\begin{aligned} \frac{1}{N} S_{u|u-1} &= \frac{1}{2\Delta H} \int_{-\Delta H}^{\Delta H} dh \int Dz \left( \beta^2 \Delta J^2 (1 - \tanh^2[\beta(h + J_0 m_{u-1} + \Delta Jz)]) \right. \\ &\quad \left. + \beta h \tanh[\beta(h + J_0 m_{u-1} + \Delta Jz)] - \log 2 \cosh[\beta(h + J_0 m_{u-1} + \Delta Jz)] \right) + \beta J_0 m_u m_{u-1} \\ &= \frac{1}{2\beta\Delta H} \int Dz \left( \beta^2 \Delta J^2 \tanh[\beta(\Delta H + J_0 m_{u-1} + \Delta Jz)] - \tanh[\beta(-\Delta H + J_0 m_{u-1} + \Delta Jz)] \right) \\ &\quad + \frac{1}{2\beta\Delta H} (\varphi(\beta\Delta H, \beta J_0 m_{u-1} + \beta\Delta Jz) - \varphi(-\beta\Delta H, \beta J_0 m_{u-1} + \beta\Delta Jz)) + \beta J_0 m_u m_{u-1}, \end{aligned} \quad (\text{B5})$$

and

$$\begin{aligned} \frac{1}{N} S_{u|u-1}^r &= \frac{1}{2\Delta H} \int_{-\Delta H}^{\Delta H} dh \int Dz \left( q_{u+1,u-1} \beta^2 \Delta J^2 (1 - \tanh^2[\beta(h + J_0 m_{u-2} + \Delta Jz)]) \right. \\ &\quad \left. - \log 2 \cosh[\beta(h + J_0 m_u + \Delta Jz)] \right) + \beta J_0 m_{u-1} m_{u+1} \\ &= \frac{1}{2\beta\Delta H} \int Dz \left( \beta^2 \Delta J^2 q_{u+1,u-1} (\tanh[\beta(\Delta H + J_0 m_{u-2} + \Delta Jz)] - \tanh[\beta(-\Delta H + J_0 m_{u-2} + \Delta Jz)]) \right) \\ &\quad + \frac{1}{2\beta\Delta H} (\varphi(\beta\Delta H, \beta J_0 m_u + \beta\Delta Jz) - \varphi(-\beta\Delta H, \beta J_0 m_u + \beta\Delta Jz)) + \beta J_0 m_{u-1} m_{u+1}, \end{aligned} \quad (\text{B6})$$

where we define

$$\varphi(h, w) = h \log[1 + \exp(2h + 2w)] + \text{Li}_2[-\exp(2h + 2w)] + hw \quad (\text{B7})$$

with  $\text{Li}_s[x]$  being the polylogarithm function.



## 1. Critical points

Assuming a nonequilibrium steady state in which  $m_u = m_{u-1} = m$ , we obtain the critical point of the system by computing the non-zero solutions of the first order Taylor expansion around  $m = 0$  of the right-hand part of Eq. B1,

$$\begin{aligned} m &\approx \frac{1}{2\beta\Delta H} \int Dz \log \frac{\cosh[\beta(\Delta H + \Delta Jz)]}{\cosh[\beta(-\Delta H + \Delta Jz)]} \\ &\quad + \frac{1}{2\beta\Delta H} \int Dz (\tanh[\beta(\Delta H + \Delta Jz)] - \tanh[\beta(-\Delta H + \Delta Jz)]) \beta J_0 m \\ &= \frac{1}{\Delta H} \int Dz \tanh[\beta(\Delta H + \Delta Jz)] J_0 m, \end{aligned} \quad (\text{B8})$$

This equation yields the self-consistent equation whose solution gives the critical inverse temperature,  $\beta_c$ :

$$\frac{\Delta H}{J_0} = \int Dz \tanh[\beta(\Delta H + \Delta Jz)]. \quad (\text{B9})$$

In the special case where  $\Delta H = 0$ , the the expansion around  $m = 0$  results in

$$\begin{aligned} m &\approx \int Dz \tanh[\beta(\Delta Jz)] + \int Dz (1 - \tanh^2[\beta(\Delta Jz)]) \beta J_0 m \\ &= \int Dz (1 - \tanh^2[\beta(\Delta Jz)]) \beta J_0 m, \end{aligned} \quad (\text{B10})$$

The critical value  $\beta_c$  is given by the solution of the equation,

$$\frac{1}{\beta J_0} = \int Dz (1 - \tanh^2[\beta(\Delta Jz)]). \quad (\text{B11})$$

Similarly, we can find the critical value of  $\Delta J$  at the limit of zero temperature by solving the equation in the  $\beta \rightarrow \infty$  limit:

$$\frac{1}{\Delta H} \int Dz \text{sign}[(\Delta H + \Delta Jz)] J_0 = 1. \quad (\text{B12})$$

## 2. Critical exponents

We can characterize some critical exponents of the system using the normalized inverse temperature  $\tau = -\frac{\beta - \beta_c}{\beta_c}$ . We first note that point the first order Taylor expansion of the following term around the critical  $\beta_c$  yields

$$\begin{aligned} \frac{1}{\Delta H} \int Dz \tanh[\beta(\Delta H + \Delta Jz)] J_0 &\approx 1 + \frac{1}{\Delta H} \int Dz (1 - \tanh^2(\beta_c(\Delta H + \Delta Jz))) (\Delta H + \Delta Jz) J_0 (\beta - \beta_c) \\ &= 1 - K'(\beta - \beta_c). \end{aligned} \quad (\text{B13})$$

We also note that the value of  $m$  around  $\beta = \beta_c$  with the third order Taylor expansion is given as

$$\begin{aligned} m &\approx \frac{1}{\Delta H} \int Dz \tanh[\beta(\Delta H + \Delta Jz)] J_0 m \\ &\quad - \frac{1}{3\beta\Delta H} \int Dz \tanh[\beta(\Delta H + \Delta Jz)] \{1 - \tanh^2[\beta(\Delta H + \Delta Jz)]\} (\beta J_0 m)^3 \\ &= (1 - K'(\beta - \beta_c))m - K''m^3 \end{aligned} \quad (\text{B14})$$

from which we obtain

$$m \propto (\beta - \beta_c)^{\frac{1}{2}} \quad (\text{B15})$$

Thus we have a critical exponent  $\frac{1}{2}$ , which is consistent with the scaling exponent of the order parameter of the mean-field universality class, which typically denoted by the symbol ' $\beta$ ' in the literature.

Similarly, we can compute the susceptibility to a uniform magnetic field  $B$  added on top of  $H_i$ , having that

$$\begin{aligned}\left.\frac{\partial m}{\partial B}\right|_{B=0} &= \frac{1}{2\beta\Delta H} \int Dz \{ \tanh[\beta(\Delta H + \Delta Jz)] - \tanh[\beta(-\Delta H + \Delta Jz)] \} \left( \beta + \beta J_0 \left.\frac{\partial m}{\partial B}\right|_{B=0} \right) \\ &= \frac{1}{\Delta H} \int Dz \{ \tanh[\beta(\Delta H + \Delta Jz)] \} \left( 1 + J_0 \left.\frac{\partial m}{\partial B}\right|_{B=0} \right)\end{aligned}\quad (\text{B16})$$

which evaluated for the limit  $\tau \rightarrow 0$

$$\left.\frac{\partial m}{\partial B}\right|_{B=0} = (1 - K'\tau) \left( \frac{1}{J_0} + \left.\frac{\partial m}{\partial B}\right|_{B=0} \right) \quad (\text{B17})$$

$$\left.\frac{\partial m}{\partial B}\right|_{B=0} \propto \frac{1 - K'\tau}{\tau} \approx (-\tau)^{-1} \quad (\text{B18})$$

retrieving the  $\gamma = 1$  exponent that is consistent with the mean-field universality class.

### Appendix C: Comparison with the equilibrium SK model

To illustrate distinct behaviours between the symmetric and asymmetric SK models, we compare the order parameters of the asymmetric SK model with the equilibrium SK model. We use the replica-symmetric solution of the model [12], which becomes unstable for the spin-glass phase but still yields an approximate phase space of the system. Figure S1 displays the phase space of the order parameters of an equilibrium SK model, which is equivalent to Fig. 2 of the nonequilibrium SK model in the main text.

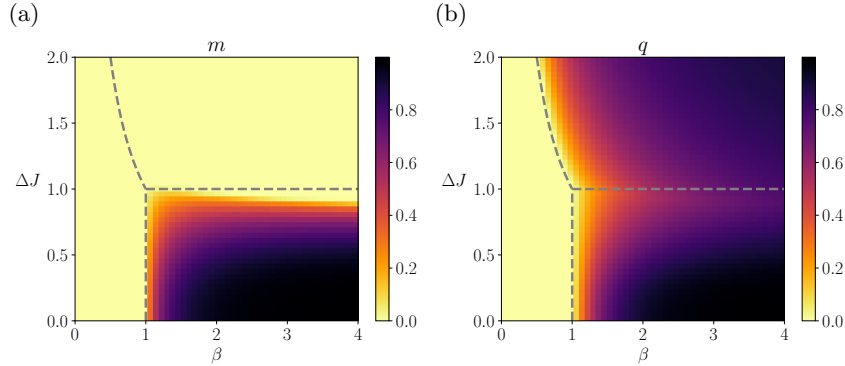


FIG. S1. **Order parameters of the equilibrium SK model with zero fields.** An approximate solution of the model with symmetric couplings is calculated under the replica-symmetry assumption [12]. The average magnetization  $m$  and the average delayed self-coupling  $q$  are shown for a model with fixed parameters  $J_0 = 1$ , and  $\Delta H = 0$  and variable  $\Delta J$  and  $\beta$ . The dashed line represents the critical line separating disordered (left), ordered (bottom-right) and spin-glass (top-right) phases.

### Appendix D: Convergence times

Spin glasses show a particular slow decay functions, which converge non-exponentially following a non-trivial slow function [52]. This finding is replicated in models like the equilibrium SK model [53, 54]. In order to refute the existence of a spin-glass phase with such slow non-exponential decay, we simulated the convergence of the average magnetization as the dynamics reaches a nonequilibrium steady state. Using the critical inverse temperature  $\beta_c$  for  $\Delta J = 0.2, \Delta H = 0$ , we use 11 values of  $\Delta J$  uniformly distributed in the interval  $[0.19, 0.21]$ . In Fig. S2, we observe, at the critical value ( $\Delta J = 0.2$ , black line), the convergence of magnetization follows a power law, as expected. Conversely, both the ordered and disordered phases ( $\Delta J < 0.2$ , blue,  $\Delta J > 0.2$ , red) converge as exponential functions. These results confirm that the disordered phase is not a spin-glass phase, as spin glasses show a non-exponential slow decay characterized by a non-trivial function.

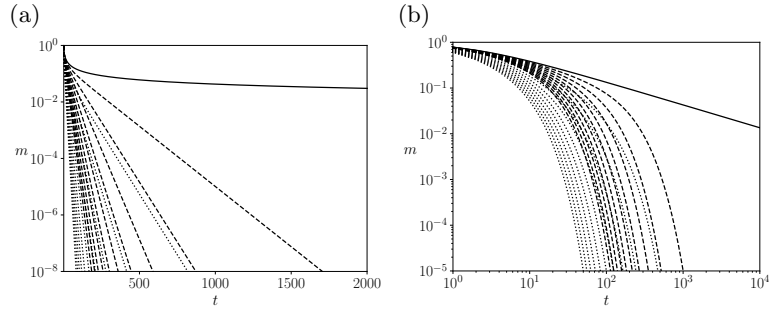


FIG. S2. **Convergence time.** Convergence times at the critical point (black), ordered phase (dotted line) and disordered phase (dashed line). All lines show an exponential decay, except for the system at criticality, which shows a power-law decay. We can know that the disordered phase is not a spin-glass phase due to the exponential decay.